PN-ABQ 103
24715
C7-14

BI-MODAL EOLIAN DESERT SAND SHEETS AND THEIR POTENTIAL SIGNIFICANCE FOR AGRICULTURAL DEVELOPMENT

FINAL REPORT

Haim Tsoar
Department of Geography
Ben-Gurion University of the Negev
Beer Sheva
Israel

Kofi Anane-Fenin
c/o Mr Emmanuel T. Adarkwa
Ghana Education Service
P O.Box M 45
Accra
Ghana

February 15, 1993

INTRODUCTION

Aim of research

The aim of this research is to enhance knowledge and understanding of spatial, dynamic, textural and chemical aspects of bi-modal sand sheets, and their potential for agricultural exploitation. It involves the use of already existing methods for studying uni-modal sands and the usufruct of practical experience gained, predominantly in Israel with dune sand agriculture on bi-modal sand sheets under different environmental conditions This research is basic in nature to some extent, but the results can serve as an important background for developing new methods of agriculture technology.

Collaboration with the LDC co-investigator

The LDC co-investigator of the project is Prof. Kofi Anane-Fenin of the University of Cape Coast in Ghana. Prof. Tsoar first met Prof. Anane-Fenin at a workshop on physics of desertification in Trieste, Italy, in 1980. There we had a long discussion on the problem of desertification and its effect on sand dune dynamics and dune sand texture change that effects the dynamic processes. These processes have a great impact on the sub-Saharan countries. The idea was that Prof. Anane-Fenin will contribute his scientific experience in his profession, which is in physics and meteorology, but mainly will learn the innovative methods of research that are performed during this investigation.

At the beginning of the research, Professor Anane-Fenin change his residence from Ghana to Liberia, where he was appointed professor of meteorology at the University of Liberia. While he was in Liberia, we had a good communication channel. Professor Anane-Fenin went to Senegal (the field area) twice.

Professor Anane-Fenin visited Israel on November 1989. The purpose of his visit was four-fold.

1. to meet, discuss and prepare with Prof. Haim Tsoar and Dr. Hendrik Bruins the field trip to Senegal planned for March 1990.
2. to take part in wind-tunnel experiment work.
3. to take part in field trips in the Negev desert.
4. to give some lectures.

The first meeting in his visit was with Prof. Haim Tsoar and Dr. Hendrik Bruins to discuss the planned field trip to Senegal. The discussion centered around equipment and transportation to and from the field site in northern

Senegal. An important and intriguing visit was to the laboratories of the Geography Department at Ben-Gurion University. Of particular interest was the visit to the granolumetry laboratory in which the various equipment for analyzing grain-size are located Professor Anane-Fenin was involoved with the wind tunnel experiments on bi-modal sand. He learned about the requirements needed for sand modeling, such as geometrical similarity, the creation of a well-developed boundary layer and the dynamic similitude maintained at appropriate scaling of all the variables which affect sand transport In order to meet these demands the tunnel was provided with a grid for generating wind profiles Measurements of wind profiles indicates that a thick boundary layer was formed. Special sand traps were designed for collecting sand in the experiments on the movement of bi-modal sands.

Professor Anane-Fenin took several field trips in the Negev. The first one was to the Nizzana dunefield The purpose of the trip was to study the morphology of the sand dunes, to have the first experience with stabilized dunes and dunes that were overgrazed by the Bedouin, and to collect sand samples. In these trips the co-investigator learned the importance of sand texture for determining sand transport by wind, the morphology of the dunes and the effect on the rate of infiltration of rainwater and on soil moisture availability for plants. Stabilization of dunes was of special interest, especially biological stabilization by perenial grass and shrub and biogenic crust. The contrast between the vegetation cover in Sinai (Egypt) and the Negev demonstrated the result of trampling and overgrazing.

Also of special interest was theuse of modern agricultural techniques on desert sand dunes that Professor Anane-Fenin saw in a number of Moshavim and Kibbutzim Since desert dune sand is an inert soil with low field capacity, agricultural cultiviation is carried by geophonics in which water and fertilizers are supplied jointly to the soil. This is done most successfuly by the trickle irrigation.

A very interesting visit was made to the Run-off Farm that was founded more than 30 years ago by Prof. Evenari. This trip was led by Dr. Pedro Berliner of the Institute for Desert Research who explained the agricultural methods used to recreate and improve the rainfall harvesting systems developed by the Israelites and continued by the Nabateaus and Byzantines 2500 to 1200 years ago. The main site for this research is the Abvdat farm located 55 km south of Beer Sheva in an arid area with an average of 80 mm of annual rainfall The other site is the Wadi Mishash farm 20 km south of Beer Sheva with 115 mm of annual rainfall.

In a short visit to the Institute of Desert Research of Ben-Gurion University in Sde Boker, Professor Anane-Fenin met some of the scientists there such as Dr. Hendrik Bruins and Prof. Avraham Zangvil of the Desert Meteorology Unit. He was also introduced to Dr. Zvi Offer who works on the

relationship between the meteorological parameters and air dust in desert conditions (deflation, transport, sedimention, aerosols and atmospheric pollution). Other visits were to the Applied Solar Calculations Unit and the Desert Architecture Unit.

As a result of violent unrest in Liberia in 1990, Professor Anane-Fenin was completely cut off from the outside world during most of the second half of that year As a result, we had to postpone the second field work which had been planned for the end of 1990 Professor Anane-Fenin managed to escape from Liberia to Ghana at the end of 1990, happily without any mishap, and at the beginning of 1991 he spent several months at the UNESCO International Center for Theoretical Physics in Trieste, Italy, before returning to Ghana, this time without a permanent address or affiliation to any scientific institute

Difficulties in conducting field work

Part of the work was conducted in the field and part in the Laboratory. The best field of sand sheets in the sub-Saharan area is located in Mali. The field work was originally planned to be carried out in the sand sheets of Mali, but because of difficulties in getting entry visas to Mali, we decided to do the field work in northern Senegal. At the beginning of the project we got in touch with Dr. Christian S. Diatta, the Director of the Institute of Applied Nuclear Technology (ITNA), Cheikh Anta Diop (C.A.P.) University in Dakar, Senegal, who had expressed his wish to participate in the project, together with three other scientists of the same institute from the disciplines of biology, physics and geology.

In May 1987 the Consul General of Senegal in Paris assured Prof. Tsoar that a visa to visit Senegal would be provided any time as needed. This promise was accompanied with a letter sent to Prof. Tsoar on June 3, 1987 (see Appendix 1). An attempt to materialize this pledge for a visa to Senegal was made in May 1988, when we planned the first field work with Kofi Anane-Fenin and three other scientists of C.A.P., University in Dakar, from the disciplines of biology, physics and geology. However, this visit to the area failed because the Consul General of Senegal in Paris reneged on his former promise and refused to grant Prof. Tsoar a visa entry. So, the first attempt to go to the field failed in spite the expenses we had for Prof Anane-Fenin's travel from Liberia to Senegal and Prof. Tsoar's travel to Paris.

Dr. Christian S. Diatta, who is our local collaborator at the University of Dakar, has met with the Senegalese Minister of Interior, who promised him solemnly that we would soon get our visas, but this promise has not been accomplished In 1990, when we felt that there was no solution to this problem, Dr. Diatta suggested that we send someone else who possesses a

non-Israeli passport to fulfil Prof. Tsoar's capacity in the field work. Our best choice was Dr. Hendrik Bruins of the Institute of Desert Research of Ben-Gurion University of the Negev Dr. Bruins is an expert on desert environment and agriculture and has a Dutch passport, with which he can easily get an entry to Senegal.

At that time we had bad communications with our collaborator in Senegal, Professor C.S Diatta, in spite of the fact that we had written him several times. Before the first field trip, he sent us, on January 18 1990, a list of field expenses (see enclosed in Appendix 2) that comes to the total of $47,000-much above the grant allocation for the collaborators in the LDC. While we were in Senegal with the aim of working in the arid area of the Ferlo region, we had long meetings in Dakar over three days with Professor Diatta, during which he wished us to clarify his position in the project Only after we had promised to make a reasonable per diem payment to three individuals from his Institute to accompany us in the field did he seem to be satisfied In order to save time and money we decided to end our contact with Dr Diatta and the second field trip was carried out by Dr. Bruins and Prof. Anane-Fenin alone without the help of any local collaborator. For that reason we could not conduct measurements in the field of northern Senegal as we had planned to do.

It transpired that we had to dedicate most of our time and energy in overcoming problems that ensuing from working in an LDC. This brought us to the idea that the problem of desertification in the sub-Saharan countries is above all a political problem and therefore can be solved in political ways. There are many political anomalies in the sub-Saharan African countries, and refusal to support research on sand sheets and their potential for agricultural exploitation, potentially useful research for these countries, is among the strange realities which any relief and help groups need to face. The lesson that we learned is that field work is impossible in these countries unless you have interested and supporting colleagues there who see the merit and importance of the research and are not primarily interested in personal benefits.

Methods:

The project was planned to be accomplished in two ways: field work, and analysis and simulation in the laboratory As was mentioned above, the field work was conducted in Northern Senegal and the the simulative laboratory work was conducted, as scheduled, in the wind tunnel of the laboratory of geomorphology of Ben-Gurion University of the Negev.

Arrangements for field work

For the field work we have purchased satellite images of Spot Image

taken on 24 March 1986 which have a resolution of 10 meters. Analysis of these images revealed a vast sand sheet field in northern Senegal, south and east of the village of Dagana (Figure 1), in an area with an average annual rainfall of about 300 mm The area is known to be composed of "subdued ancient erg dunes" that suffered from overgrazing and firewood collecting during the last 20 years Several low subdued dunes have developed in this area. The area has gradually deteriorated and degenerated from an ecological point of view, but it can nevertheless serve as a good field site for sand sheet studies.

Field work was originally planned to be carried out after field equipment such as sand traps, anemometers, wind recorders etc., are sent to Senegal, and the necessary arrangements are made for field work with Dr. Diatta and his staff However, as mentioned above it was very difficult to communicate and impossible to collaborate with scientists from Senegal. For that reason the field work only included two trips to area, First one on March 1990 and the second on December 1991. In these two trips we took samples of sand for grain-size, mineralogical, SEM, and dating analysis. Dynamic measurements of wind shear stress, sand flux and dust deposition could not be performed because of difficulties in frank collaboration with the Senegalese scientists, as elaborated above.

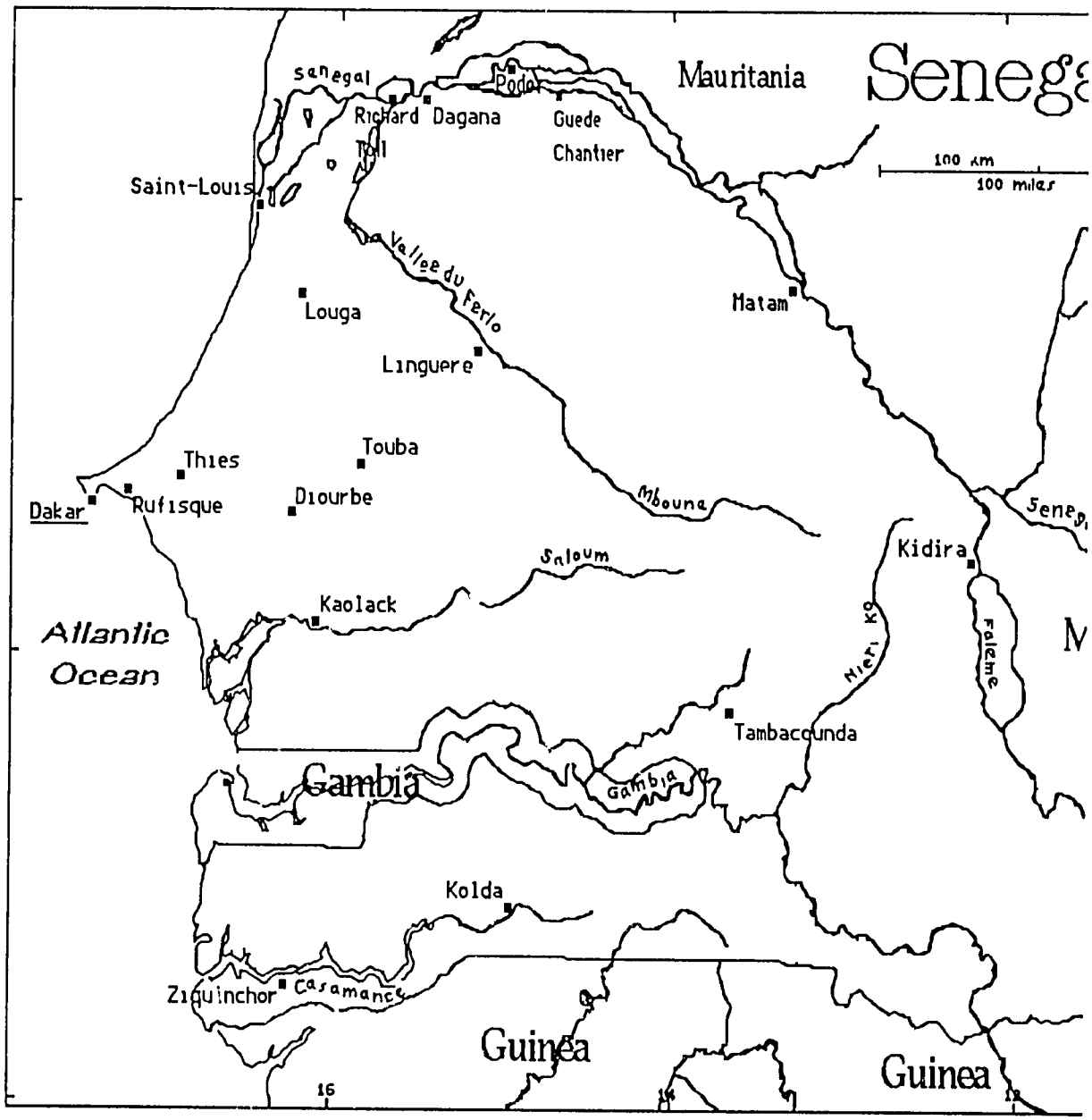

Figure 1: The research area of Senegal.

THE RESEARCH FIELD AREA

The area chosen for the field work is located in northern Senegal, known as the Ferlo region (Figure 1) It is bounded in the north and east by the Senegal River, to the west by the Lac de Guiers, and to the south by the road leading from Louga through Linguére to Matam This area is located between the Sahara desert and the humid tropical climates and is known to have had major climatic variations during the Upper Pleistocene and the Holocene. These climatic change events are reflected in the character of the eolian sand deposits of the area

Northern Senegal sustained a humid period between 40,000 and 30,000 B P.; when the dunes constituting the ancient erg of Ferlo became subdued in form and underwent soil formation. A change to an arid period occurred

between 20,000 and 12,000 B.P The massive dunefields which occupy western Senegal in the region of Cayor were formed at the height of this arid period. These sand seas, known as the Ogolian, have been emplaced over more than 500 km along the shores of the Atlantic Ocean, from southern Mauritania to Senegal The dunes consist of fine to medium sand which, according to Michel (1980), have been transported over only short distances by the wind. Following the arid period, there was a humid phase from 11,000 to 8,000 B P , when the dunes were stabilized by savanna vegetation and were characterized by reddish sands. Red-brown soils have developed on the stabilized dunes. During the last few millennium, the climate was humid with minor variations of dry climates There was a minor dry phase around 2,000 B.P. and the Middle Ages was characterized by relatively humid conditions (Michel 1980).

The average annual rainfall of the area during the period 1920 to 1969 varied from 320 mm in the north to 520 mm in the south. The rain comes in a monsoonal regime between July and October (Griffiths & Soliman 1972). During the 15-year drought of 1970-1984, the rainfall fell at 60% of its former level on average, with not a single year reaching the 1920-1969 average (see Figure 3). The average precipitation for Guede Chantier near Podor (16^0 27'N, 14^0 39'W) for the period 1970-1986, is 171 mm (data given to me by courtesy of Ms. Jane Rossing of N'Dioun). Figures 2, 3 & 4 depict the analysis of the rain data and indicate that, within the decrease of 50% in the average annual rainfall, there is an increased rainfall during the period of November to March.

Mean annual temperatures vary from the maximum of 35 to 37°C to a minimum of 19 to 21°C, with May being the hottest month and January the coldest Annual potential evaporation varies from about 1675 mm to 2100 mm.

In the Ferlo, as in the Sahel as a whole, the more northerly vegetation can be described as sparse *Acacia* thorn tree scrub, while in the southern part, *Combretum* and baobab trees become dominant. *Balanites agyptiaca,* the "desert date," is common in both zones.

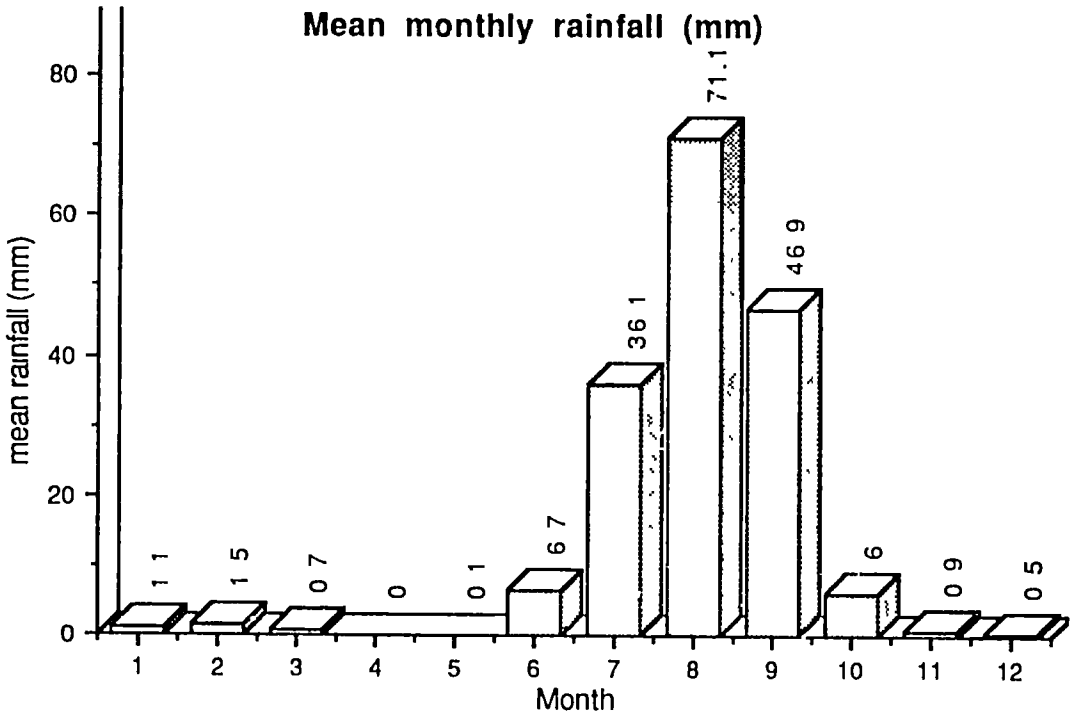

Figure 2: The mean monthly rainfall of Guede Chantier, northern Senegal, for the period 1971-1986.

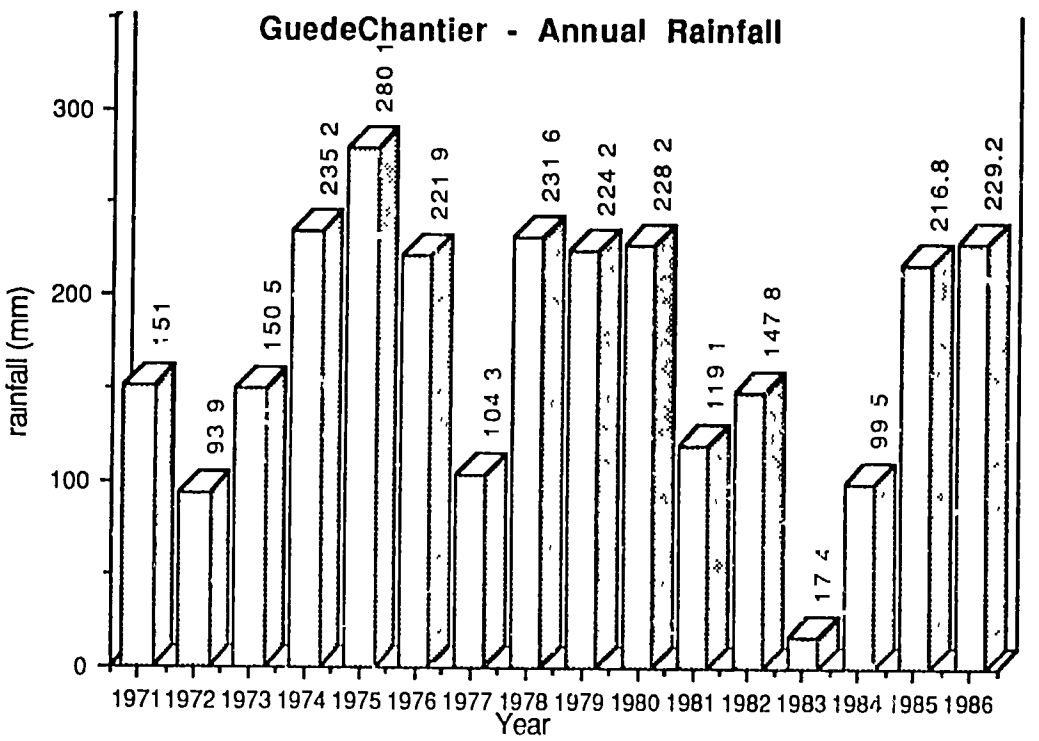

Figure 3. The distribution of northern Senegal annual rainfall (in percent) for the period 1971-1986.

The Ferlo is occupied mainly by Fulani semi-sedentary pastoralists numbering approximately 90,000. Toucouleur agriculturalists live in the Senegal River valley and around some of the larger boreholes. Maure pastoralists commonly enter the Ferlo in the dry season from Mauritania, bringing with them thousands of cattle, camels, sheep and goats, putting increased pressure on the grazing resources at the most sensitive time The human population density in the Ferlo is about three persons per km^2, one of the lowest in the Sahel, though distribution is not even. This relatively low population density, along with only recent water development, partly explains the comparatively good ecological conditions found in the Ferlo in relation to the rest of the Sahel. Rainfed agriculture is practised by the people living along the Louga - Linguére road, and there are signs that land clearance and barren fallow fields are leading to more severe degradation than seen in the purely pastoral areas.

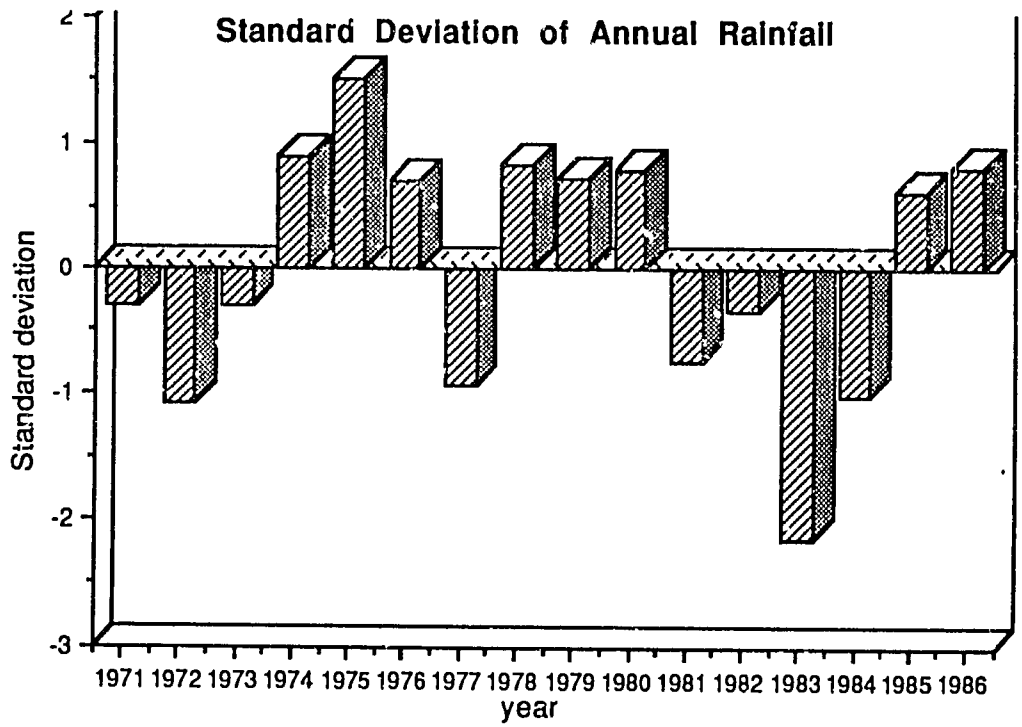

Figure 4: The deviation of northern Senegal annual rainfall from the mean (1971-1986).

Prior to 1950, the Ferlo had no permanent water and it was referred to as a "desert." Some of the Fulani would move into the central and southern Ferlo during the rainy season, about July or August, and remain with their herds until the rain pools and dug-out reservoirs dried up in October or November. Others would trek north with their herds into Mauritania to search out the highly nutritious grasses found on the sand dunes They would all then retreat back to the Diéri and Walo zones for the long dry season.

Between 1950 and 1980, some 35 deep boreholes and 33 drilled wells were installed in the Ferlo Permanent water transformed land use patterns and today one can find groups of Fulani settled more or less permanently around the more reliable boreholes and wells. Almost all of the people and livestock moved out of the Ferlo, however, in 1972 and 1983-1984 due to drought-induced lack of forage. Because of no proper management, the excess of water acts as an ecologically destabilizing factor by encouraging the growth of herds and human populations beyond the limits of the range to support them

This naturally produced change in the ecological conditions has left its impression on the area. An analysis of satellite images by Spot Image, taken on 24 March 1986, revealed vast fields of sand sheets that suffered from overgrazing and firewood collecting during the last 20 years, which has led to the development of several low active dunes The area has gradually deteriorated and degenerated from an ecological point of view -- a process known as desertification

LABORATORY WORK

In the laboratory we have prepared a boundary-layer low-speed wind tunnel appropriate for studying the movement of the coarse sand of which sand sheets are composed The wind tunnel of Ben-Gurion University of the Negev is an open circuit tunnel and is composed of three parts: entrance cone, test section and diffuser. Air is sucked in through a bell-shaped entrance by a fan located at the end of the diffuser. In that way, disturbances of air flow inside the tunnel that could result from the rotating fan are kept at a minimum. This gives an advantage to this wind tunnel over the blower type

It is important to ensure that conditions in the wind tunnel are representative of natural full-scale conditions. If criteria of similarity permit modelling, then wind tunnel simulation offers many advantages over field work, such as: detailed study of controlled conditions, rapid research, low cost, access to a high versatility of flow conditions and grain-sizes, and easy emplacement and replacement of measuring sensors. The penalty is that studies of any effects of an intrusive body usually have to be done at reduced scale.

Special requirements are needed for the flow conditions to guarantee similitude of tunnel airflow, blown sand and static models with natural full-scale conditions (Cermak 1971) Important requirements for sand and dune modelling are:

(a) The model should be geometrically similar and scaled to be a true

prototype;

(b) The vertical velocity profile shape and the level of turbulence of the boundary-layer should equal real atmospheric flow conditions;

(c) The test section should be long enough to perform sand transport at a uniform rate;

(d) Dynamic similarity through the observance of applicable dimensionless similitude parameters should be ensured.

Geometric similarity for simulated static dunes or obstacle models is achieved when all linear dimensions of the model relate to corresponding dimensions of the prototype in a constant scale factor (Tsoar 1983b) This requirement might be difficult or impossible to achieve with the size of the test section

Simulation of the atmospheric boundary-layer in a wind tunnel can be performed when the roughness parameter for the tunnel floor accords, according to scale, with the roughness parameter corresponding to nature (Jensen 1958).

$$Z_{om}/Z_{op} = L_m/L_p$$

Am explanation of symbols appears in Table 1. Subscript m denotes the model variable and p the prototype.

A thick wind tunnel boundary-layer grows naturally by roughening the floor on a great length upstream of the test section. This requires a very long wind tunnel with a long fetch ahead of the test section. Such a naturally grown boundary-layer with sufficient depth has an excellent agreement with atmospheric data (Cook 1978). Short wind tunnels such as the one at Ben Gurion University of the Negev, however, allow for a thick boundary-layer to be formed by a velocity-profile generator. Here velocity can be non-uniformly reduced by placing, ahead of the test section, a closely graded grid of rods near the floor which becomes more widely spaced close to the roof (Cowdrey 1967).

Equilibrium of the boundary layer with the sand it transports is achieved more slowly than the development of the sand free boundary layer. The length required for the test section depends to a marked degree on the type of sand with which experiments are performed For dune sand, such conditions can be obtained at the downwind end of a test section that is 10 to 15 metres long (Bagnold 1941, p. 26). The test of adequate length is to observe whether, in the absence of obstructions in the tunnel, an initially flat bed of free sand remains flat without change in depth in the test section of the tunnel

Conditions for dynamic similarity can be established best by considering

all variables which affect the drag on a body (model) put in the wind tunnel. Important variables involved in sand transport and dune models are presented in Table 1.

Table 1: Variables involved in wind tunnel simulation work of aeolian processes, the dimensions of each variable are indicated in parenthesis.

u - velocity in the boundary-layer ($L\ T^{-1}$)
u_∞ - velocity outside the boundary-layer ($L\ T^{-1}$)
u_* - friction velocity ($L\ T^{-1}$)
u_{*t} - threshold friction velocity ($L\ T^{-1}$)
w_f - settling velocity of grains ($L\ T^{-1}$)
g - acceleration due to gravity ($L\ T^{-2}$)
ρ_f - fluid density ($M\ L^{-3}$)
ρ_s - grains density ($M\ L^{-3}$)
γ - specific weight of sand in bulk ($M\ L^{-3}$)
μ - dynamic viscosity of fluid ($M\ L^{-1}T^{-1}$)
ν - kinematic viscosity of fluid ($L^2\ T^{-1}$)
L - size of model as specific to some characteristic dimension (L)
Zo - surface roughness (L)
d - grain diameter (L)
δ - boundary-layer thickness (L)

Having knowledge of the variables that affect the air and sand motion in the wind tunnel, it is possible to combine variables into dimensionless groups regardless of the values of individual variables in that group. In this way, the total number of variables in Table 1, which must be experimentally varied, is reduced into several dimensionless variables (Kline 1965, p. 17). The *Buckingham Pi Theorem* is one method of identifying a competent number of dimensionless groups to define a problem (Buckingham 1914).

In non-compressible fluid mechanics, such as airflow in a low-speed wind tunnel, there are three primary dimensions (Table 1): L, M, and T. Table 2 shows some variables selected for dimensional analysis. n is the number of variables (n=5), and r is the number of the primary dimension (r=3).

Table 2: Set of variables and their dimensions

r	ρ_f^a	u^b	d^c	μ	ρ_s
M	1	0	0	1	1
L	-3	1	1	-1	-3
T	0	-1	0	-1	0

A number of n-r equations can be set up by combining parameters selected from Table 2 to form dimensionless groups of Π. According to Table 2, one dimensionless group is.

$$\Pi_1 = \rho^a_f \; u^b \; d^c$$

$$\Pi_1 = (M/L^3)^a \; (L/T)^b \; L^c \; M/LT = 0$$

The exponents of the variables are equated from Table 2:

M: a+1=0

L: -3a+b+c-1=0

T: -b-1=0

The solution is: a=-1, c=-1 b=-1. A dimensionless Π_1 group can be set up as

$$\Pi_1 = \mu/\rho_f \; d \; u|_{model} = \mu/\rho_f \; d \; u|_{prototype}$$

The second dimensionless group (according to Table 2) is:

$$\Pi_2 = \rho^a_f \; u^b \; d^c \; \rho_s$$

$$\Pi_2 = (M/L^3)^a \; (L/T)^b \; L^c \; M/L^3 = 0$$

The exponents of the variables are equated from Table 2:

M: a+1=0

L: -3a +b+c-3=0

T: -b=0

The solution is: a=-1, b=0, c=0. A dimensionless Π_2 group can be set up as:

$$\Pi_2 = \rho_s/\rho_f \,|_{model} = \rho_s/\rho_f \,|_{prototype}$$

It is often impossible or impracticable to reach a simulataneous satisfactory dynamic similarity of all parameters. For example, Reynolds Number and Froude Number are often achieved popular dimensionless parameters, but can never both be matched on a range of velocities. When static models are used, it is impossible to arrive at matching conditions between model and full-scale-size parameters because L of the model is scaled down by between 1.50 and 1 200 (Kind 1976, Kind & Murray 1982). It is more important, however, to get a fully developed turbulent flow; a strict matching of Reynolds Number is not always necessary for dynamic similarity (Mirener 1979, p. 330). A fully developed turbulent flow requires that the roughness Reynolds Number ($U_* z_0/\nu$) be larger than 2.5 (Isyumov & Tanaka 1980) This may be difficult to achieve if the scale of the roughness parameter in the model is adhered to. The level of turbulence has an important influence on the mode of particle movement and also the separation and reattachment characteristics of the flow (Jensen 1958).

There are some physical limitations to dynamic similarity because not all variables can be changed without a drastic concomitant change in the characteristics of particle movement. For instance, if grain-size or density is reduced to such low values that the particle might be affected by the vertical component of the turbulence, it may well be transported in suspension instead of by saltation. The ratio of grain density to fluid density determines the character of the saltation. When this ratio is about 2000 (as it is for quartz grains in air) the character of saltation is completely different than it is in water, where the ratio is about two (Bagnold 1941, p. 163). Hence, simulation of wind-induced saltation in water is not possible (Kind 1976).

In conclusion, maintaining simulation conditions for small scale models of sand transport is sometimes problematic because of the large number of variables involved (Table 1) Since it is practically impossible to have all the model's dimensionless parameters match with the prototype, there is a small penalty in accuracy of modelling. Good experimental practice identifies any such "scale effect" and evaluates its effect on the conclusions of the study. With appropriate caution in interpretation, this enables valuable work to be done using wind tunnels and scale models.

Another important question is to what wind velocity in the field the wind tunnel velocity is competent It is postulated that the flow in the field and in the wind tunnel is turbulent with a developed boundary layer. Therefore, the average velocity of the wind in the wind tunnel can be matched with the speed of the wind measured on a high mast in the field. The average speed in the wind tunnel (U) can be calculated according to the ratio between the wind discharge (Q) and the cross-section area (A) of the test section:

$$U=Q/A$$

Q is achieved by calculating the integral of wind tunnel boundary layer reaching a thickness of 0.15 m

$$U=Q/A=U_*/0.4\ [\ln(\delta/z_0)-(\delta/L)]$$

where:

L = the wind tunnel width (0.7m)

δ = the height of the boundary layer in the wind tunnel (0.15m)

z_0= roughness length

The maximal sand discharge values in the wind tunnel form a very good correlation (r=0.9896) with the wind velocity, as measured at a height of 0 15m.

$$q=(0.038+0\ 0092U)^3$$

where U is the wind speed (m s^{-1}) and q is the sand discharge (m^3 min^{-1}).

Results of discharge for the various wind speeds (measured at a height of 0.15m) in the wind tunnel are shown in Table 3.

Table 3: Sand discharge values for various wind speeds (at a height of 0.15m) in the wind tunnel

wind speed (m s^{-1})	sand discharge (m^3 m^{-1} hr^{-1})
7	0.091
10	0.198
12	0.280
13	0.336
14	0.397
15	0.467
16	0.544
17	0.630
19	0.826
21	1.060
25	1.650

Field measurement with sand traps taken on coastal dunes after a severe wind storm (20 m s^{-1}, measured at height of 2 m) gives sand discharge of 2.76 m^3 m^{-1} hr^{-1}. This sand discharge is compatible with wind tunnel sand discharge for speeds of 30 m s^{-1} at a height of 0.15 m.

In conclusion, maintaining simulation conditions for small scale models of sand transport is sometimes problematic because of the large number of variables involved (Table 1). Since it is practically impossible to have all the model's dimensionless parameters match with the prototype, there is a small penalty in accuracy of modelling Good experimental practice identifies any such "scale effect" and evaluates its effect on the conclusions of the study. With appropriate caution in interpretation, this enables valuable work to be done using sand transport in a wind tunnel

The sand feeder built for the wind tunnel has eight outlet pipes so that the rate of sand discharged from the feeder can be easily measured and regulated. A test of poorly sorted coarse sand, created synthetically from sand components selected in the Negev desert, is shown in Figure 5. After 8 hours of wind speed of 10 m s^{-1}, the sand surface was stabilized by the formation of armoring coarse particles on the surface ("Tunnel sand" in Fig. 5)

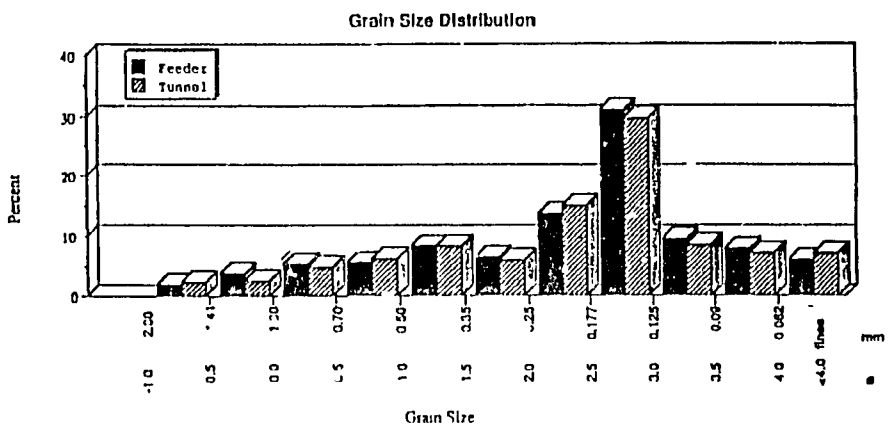

Figure 5: Grain-size distribution of poorly sorted sand. In black, the grain-size distribution given by the feeder. In grey, the tunnel surface grain-size distribution after 8 hours of wind velocity of 10 m s^{-1}.

The sand trap designed for the wind tunnel work consists of six chambers, one on top of the other, each with an aperture of 10x20 mm and a length of 350 mm (Fig. 6). The exit port at the top of the chamber is meant for decreasing the stagnation pressure and is covered by a fine mesh of 75 µm. Measurements of the amount of sand trapped by the chambers (q) in gr cm^{-1} hr^{-1} under several different wind velocities (u) show a very good correlation (r=0.994) between q and u^3 (Figure 7). According to the regression equation, $q=(0.63u-4.5)^3$, it follows that the threshold velocity

(impact threshold) for this sand, measured at a height of 15 cm, is 7.15 m s^{-1}.

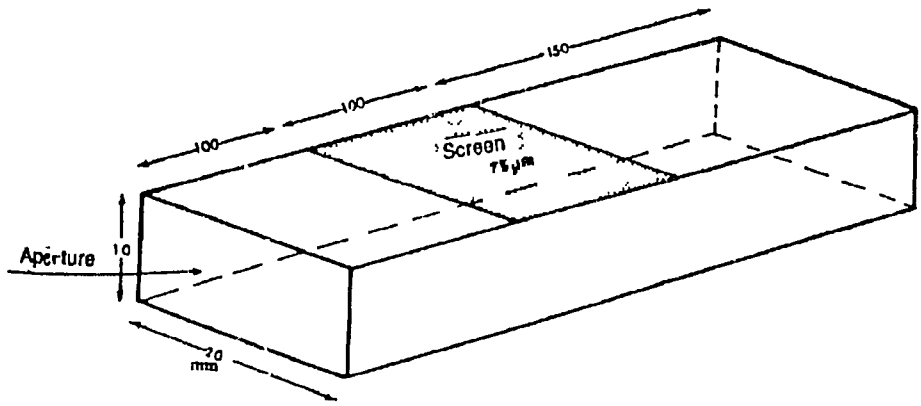

Figure 6: A chamber for trapping saltating sand

Regression line for sand transport and wind velocity

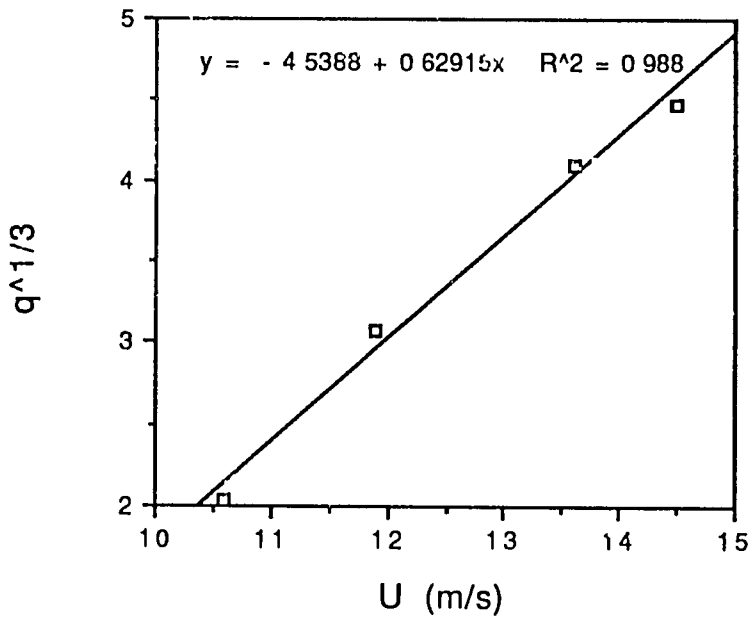

Figure 7: Regression line for the correlation between sand transport ($q^{1/3}$) and wind velocity (U).

In another wind tunnel test, the grain-size of the sand caught by the trap was compared with the surface sand grain sizes (Fig. 8). It is obvious that the trapped sand is finer than the surface sand because it contains the saltation load, whereas surface sand has a great proportion of coarse lag creeping grains. The sand used in the feeder is similar in size to sand collected in the trap

Measurements of profiles of wind velocity were taken under several

wind speeds, from the threshold velocity up to the highest possible wind tunnel speed. The threshold friction velocity (u_*) is 31 cm s^{-1} and the highest friction velocity is 111 cm s^{-1}. The roughness length (Zo) is 1.766×10^{-5} m. This corresponds to an average surface grain-size of 0.53 mm (30Zo).

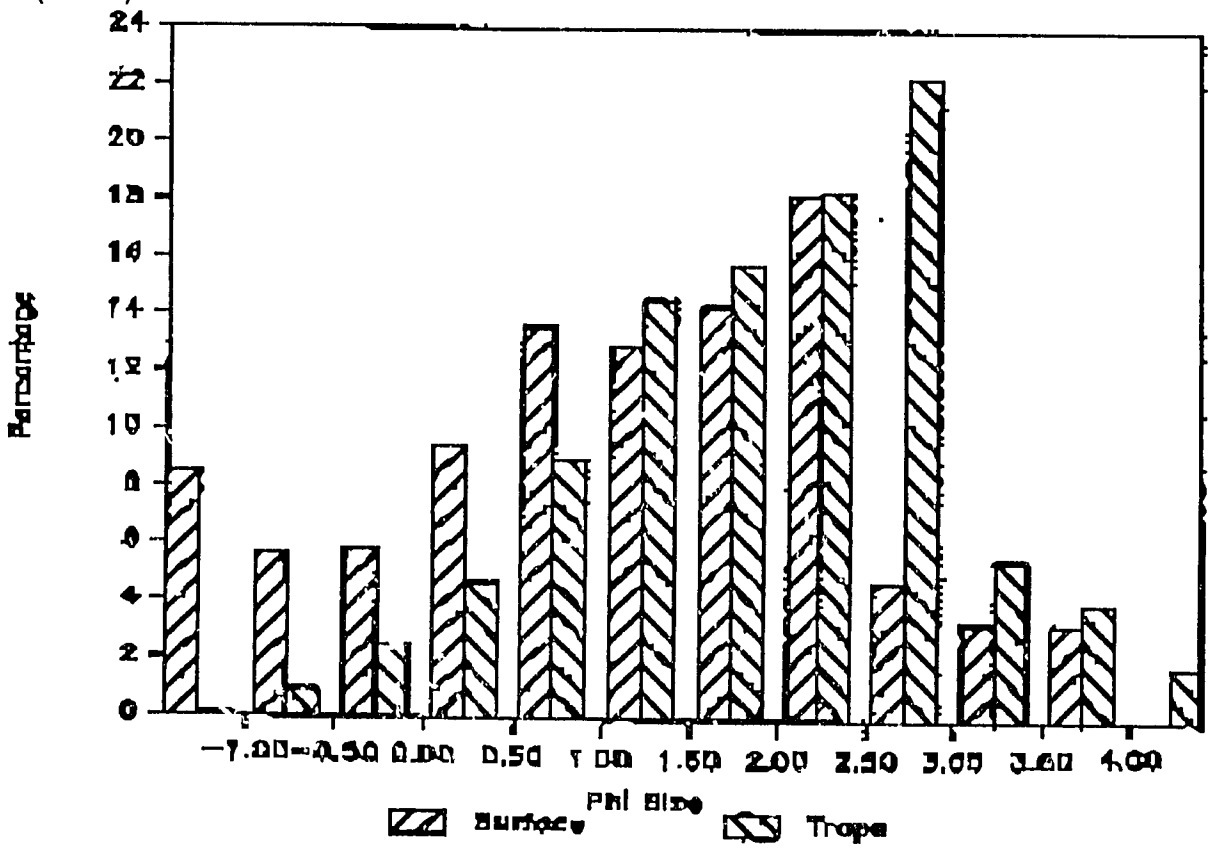

Figure 8: Comparison between grain-size distribution of tunnel surface sand and sand collected in the trap.

DUNE SAND TEXTURE

Introduction

The texture of sand is the factor that accounts for the poor vegetative vitality found on dune sand It induces low field capacity and a low value for soil moisture availability for plants, as well as a high rate of permeability and leaching resulting in the washing away of nutrient elements necessary for plant growth. The extreme mobility of loose particles of sand causes them to be easily swept away by the wind in a leaping movement which describes a ballistic path very close to the bed, a process known as *saltation* (White, 1982). This process is detrimental since the grains bombard the plants, causing them damage and disease.

Saltation is characterized mostly by grains in the range of fine sand (125-250 µm; 3-2ø; Figure 8). Suspension, which is the second major transport mode, is characterized by grains < 74µm or < 3.75ø (dust) which are carried for large distances by the windflow. The range between these two modes (74-125µm or 3-3.75ø) is of grains that display trajectories between saltation and suspension, known as *modified saltation* (Tsoar and Pye, 1987).

For the systematic analysis of this and parallel processes, a number of different classifications of soil grain-size have been devised, all based on classifying soil particles according to four systems: gravel, sand, silt, and

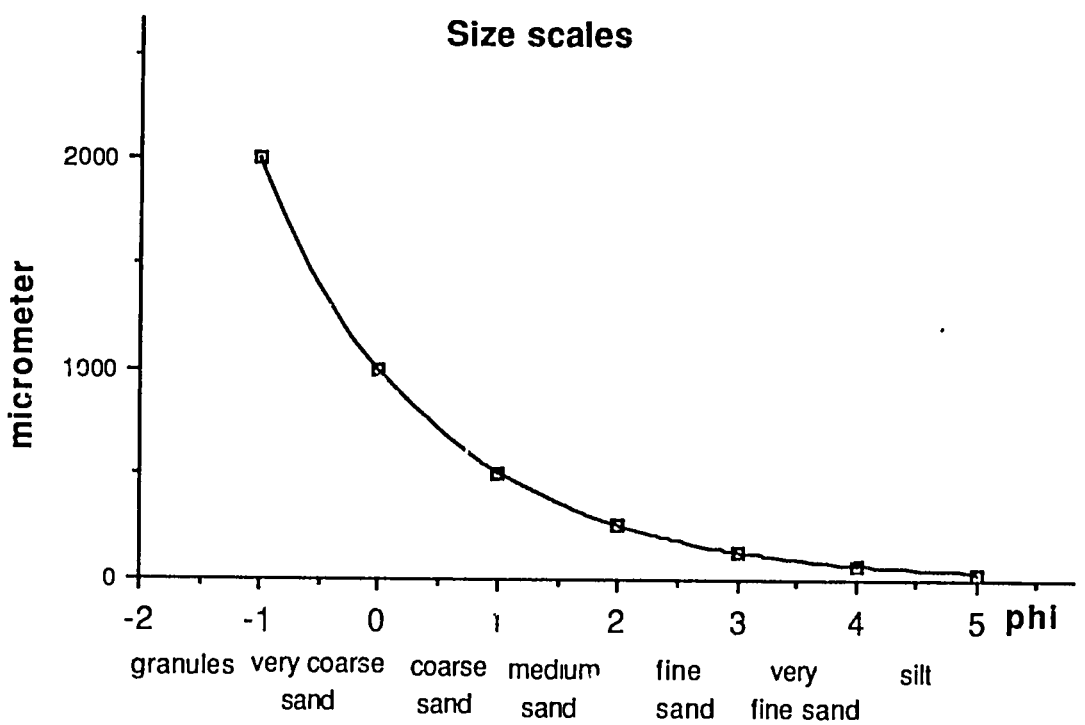

Figure 8: Relation between the phi (ϕ) scale and sizes in micrometer (µm)

clay. Figure 8 shows the classification corresponding to the grain-sizes found in the sand sheets of northern Senegal. The saltation mode corresponds to grains in the range of *fine* sand that move most easily under storm winds of average intensity. Coarser grains of *medium, coarse*, and *very coarse* types are too heavy to be driven directly by an average-force wind, but are driven forward along the surface in a creep mode through the impact of the saltating grains (Bagnold, 1941).

Particles of *very fine* sand, silt, and clay sizes are so small that they have low settling velocities relative to the velocities of the vertical component of the turbulent wind flow. As a result, these particles remain in suspension or quasi-suspension in their transportation mode and are considered as dust (Tsoar and Pye, 1987). The desert atmosphere is loaded with particles in suspension (dust). However, active desert sand dunes contain no more than 3% of particles < 74µm or < 3.75Ø (Tsoar, 1976) that easily enter into suspension mode by the impingement of the saltating grains. Nevertheless, when sand is stabilized by vegetation, the saltation is reduced and the amount of fines (<74 µm or <3.75Ø) increases at the sand surface. Rainwash leaches some of these fine particles to depths of 30-50 cm (Tsoar and Møller, 1986). The longer the dune is stabilized, the higher the content of the fines (Danin, 1978). Hence, the grain-size distribution can give a clue as to the mobility or stability of the sand dune.

The morphology of dunes is determined by the distribution of the grain-size of the sand. Sharp-edge shaped dunes, such as most seif and transverse dunes, are composed of very well-sorted modes of fine sand, whereas the plinth of dunes, interdune areas, and low flat dunes such as sand sheets and zibars consist of bi-modal sand (Holm, 1960; Warren, 1972; Tsoar 1983a, 1986).

Particles larger than sand size (>-1.0Ø) can be moved by very strong winds that normally are not found in the sub-Saharan area. Coarse sand larger than 500 µm (1.0Ø) is usually very rare in the sand sheet of northern Senegal. If this sand exists, it can be a result of aggregates or calcic grains originated from the calcic horizons developed during the period when the sand is stabilized.

In spite of the fact that sand coarser than fine sand cannot easily be transported directly by average wind storms, about 38% of the aeolian depositional surfaces (1,520,000 km^2) are composed of bi-modal sand sheets (Fryberger & Goudie, 1981). Eolian bi-modal sand of ancient sandstones and modern deserts are composed of two distinct modes, with very few grains of intermediate size (Folk, 1968). The coarse mode is always coarser than fine sand (2-3Ø), which is the mean size of desert dune sand (Ahlbrandt, 1979). The fine mode can be either in the range of fine

sand (Bagnold, 1941; Tsoar, 1978), or finer (Folk, 1968; Warren, 1972). Descriptions of extensive plains of bi-modal sand sheets are known from various parts of the world's deserts (Bagnold, 1931; Simonett, 1960; McKee & Tibbitts, 1964; Mabbutt, 1968; Folk, 1968; Glennie, 1970; Warren, 1972; Wilson, 1973; Haynes, 1982; Tsoar, 1983a). Holm (1960), describes long wavelength, low amplitude bedforms formed on sand sheets in Arabia and denominates them by the native name, *zibar* (Pye and Tsoar, 1990).

The origin of bi-modal sand sheets is obscure. Bi-modalism of wind-blown sand can be explained by repeated interaction of a saltation and a creep fraction that are almost in equilibrium. Wood (1970) developed mathematical models showing how bi-modal sand may have evolved from uni-modal sand. Bagnold (1941) and McKee and Tibbitts (1964) speculated that this coarse sand formed from periodical flooding and other alluvial deposits that were periodically reworked and winnowed by wind. However, a fluvial origin is ruled out because bi-modal sand occurs over wide desert areas without the presence of interbedded pebble beds (Glennie, 1970).

Folk (1968) discredits the interpretation that sees the bi-modality as a result of mixing of the traction load in dunes (coarse sand) with grains deposited from suspension (silt). Instead, he suggests that bi-modal sands originate by winnowing of fine and medium sand grains from poorly sorted fluvial detritus. Thus, bi-modal sediments are left behind, composed of grains which are too coarse to saltate and finer grains which pack together to form a cohesive surface.

Warren (1972) doubts this interpretation on the grounds that bombardment by saltating grains tends to entrain the finer fractions into suspension, as was observed in many soil erosion studies (cf. Chepil, 1958). Instead, he suggests a process of protection of the fine grains in the inter-particle voids between the coarse grains. The slightly coarser fraction of the saltation load, which is too large for the voids, is not protected and moves onward until it accumulates into dunes. However, neither of these hypotheses can explain the formation of bi-modal sand with one fine mode in the range of easily saltating grains (2-3Ø) which, according to Folk (1968) and others, is reported from many ancient sandstones and modern deserts.

RESULTS

About 85 samples of sand were retrieved from the field of northern Senegal during the two field trips. Most of the samples were bi-modal or multi-modal. Samples were taken from various locations during the first field trip (Table 4).

Table 4: The location and type of sand samples retrieved during the first field trip

sample #	Location	Type of sample
SE-1	34 km SW of Richard Toll	Sample of saltating sand in the air above the tiny linear dunes.
SE-2	34 km SW of Richard Toll	Bulk sand sample of the tiny linear dunes.
SE-3	34 km SW of Richard Toll	Sample of the crust on small coppice dune, east of the road.
SE-4	34 km SW of Richard Toll	Sample of darker (heavier) sand grains from the crest of the ripples on the tiny linear dunes.
SE-5	Dimar Thiewle	Sample of the coarse sand particles on the crest of the megaripples downwind from the seif dune.
SE-6	Dimar Thiewle	Sample of actively saltating, airborne sand, collected in the air downwind from the slip-face of the seif dune.
SE-7	Dimar Thiewle	Sample of sand, somewhat consolidated, of the ancient linear dune, as found in between and below the active megaripples. The ancient dune sand is stratified.
SE-8	Dimar Thiewle	Sample of sand from the active slip-face of the seif dune.
SE-9	Dimar Thiewle	Sample from upper layer (0-37 cm), which appears to be a colluvial deposit of dune sand mixed with some laterite gravel. Not visibly stratified.

SE-10	Dimar Thiewle	Sample from second layer (37-58 cm), composed of stratified and cross-bedded dune sand, whiter in color than the other layers and also least consolidated.
SE-11	Dimar Thiewle	Sample from third layer (58-125 cm), composed of more reddish and somewhat consolidated sand. Not visibly stratified.
SE-12	Dimar Thiewle	Sample from fourth layer (125-200+ cm), composed of bright reddish sand, somewhat consolidated, overlying the laterite. This lowermost sample is taken from about 180 cm depth.
SE-13	14 km NE Saint Louis	Sample of sand from active slip face on the large, southern seif dune.
SE-14	14 km NE Saint Louis	Sample of coarse sand from the crest of the megaripples downwind from the slip face of the seif dunes.
SE-15	14 km NE Saint Louis	Sample of stratified dune sand from an exposed part of the ancient linear dune.
SE-17	14 km NE Saint Louis	Surface sample with crust from the stable linear dune, situated to the northwest of the former linear dune with active seif dunes. The surface of the stable linear dune is quite extensively vegetated and a crust has formed, probably due to influx and incorporation of dust.
SE-18	3 km north of Louga	Surface sample in a typical landscape of slightly undulating coversand deposits. Some fields have been used for millet cultivation. There are also goats

		in the area. Sample from surface with natural vegetation.
SE-19	109 km south of St-Louis	Slightly undulating landscape with coversands. Many Baobab trees near a field used for millet cultivation. Other trees as well. Surface sample with a crust on the sand from below a Baobab tree.
SE-20	160 km south of St-Louis about 30 km north of Thies	Slightly undulating landscape with coversands and many trees. Many termites appear on the soil. Hence it took some time to find an undisturbed spot, from where a surface sample was taken.
SE-21	Dakar University	Surface sample with crust on the sand from the garden around the ITNA building.

During the second field trip we took mostly samples of sand from different depths, to study the soil profiles and diagenesis of the soil (Table 5).

Table 5: The location, type, and color of sand samples retrieved during the second field trip

Sample #	Depth (cm)	Location	Munsel color
SE-22	10-20	4 km north-east of Louga along the road to Niomre Lo	5YR 6/6
SE-22B	50- 55	ditto	5YR5/5
SE-23	85- 90	ditto	5YR4/5
SE-24	130-135	ditto	5YR4/6
SE-25	175-180	ditto	5YR5/6

SE-26	225-230	ditto	5YR6/6
SE-27	285-290	ditto	5YR6/6
SE-28	370-375	ditto	5YR6/6
SE-29	455-460	ditto	5YR6/6
SE-30	520-525	ditto	5YR6/6
SE-31	595-600	ditto	5YR6/6
SE-32	660-665	ditto	5YR6/6
SE-33	715-720	ditto	5YR6/7
SE-34	780-785	ditto	5YR6/7
SE-35	880-885	ditto	7.5YR6/6
SE-37	935-940	ditto	2.5YR5/7
SE-40	30-35	93 km east of Richard-Toll 29 km west of Ndioum	7.5YR4/4
SE-41	75-80	ditto	7.5YR5/4
SE-42	115-120	ditto	5YR6/6
SE-43	0-3	1 km east of Ndioum	5YR5/3
SE-43B	0-1	ditto	7.5YR5/4
SE-44	5-8	ditto	6.5YR5/4
SE-45	110-115	ditto	5YR5/4
SE-46	185-190	ditto	2.5YR5/4
SE-47	230-235	ditto	2.5YR5/5
SE-49	340-345	ditto	2.5YR5/6

SE-58	5-10	13 km south-east of Richard-Toll 4km south of Pate Badio	7.5YR 5/4
SE-59	25-30	ditto	7.5YR 5/4
SE-61	18-23	31 km south-east of Richard-Toll, 22km south of Pate Badio	10YR5/3
SE-62	0-4	40 km south/south-east of Richard-Toll, 31 km south of Pate Badio, 2 km north ofthe well of Medina Yelour.	10YR5/3
SE-63	15-20	ditto	10YR6/3
SE-64	30-35	ditto	10YR5/3
SE-65	0-5	26 km south of Dagana 17 km north-east of Medina Yelour	7.5YR5/4
SE-66	10-15	ditto	5YR5/3
SE-67	18-22	ditto	5YR4/4
SE-68	0-4	25 km south of Dagana 18 km north-east of Medina Yelour	10YR5/4
SE-69	8-14	ditto	10YR5/3
SE-70	27-32	ditto	7.5YR5/4
SE-71	0-4	14 km south of Dagana	9YR5/4
SE-72	18-23	ditto	7.5YR5/4

SE-73	0-4	26 km east of Richard-Toll 5 km east of the western Dagana intersection, about 3 km south-east of Dagana	7.5YR5/4
SE-74	7-11	ditto	5YR5/6
SE-75	13-19	ditto	7.5YR5/4
SE-76	28-34	ditto	5YR4/4
SE-77	4-9	Ndiayene 74 km east of Richard-Toll.	7.5YR5/4
SE-78	23-28	ditto	7.5YR5/4
SE-79	sand of active slip-face of seif dune	ditto	5YR 6/6
SE-80	20-25	ditto	5YR 5/6
SE-81	50-55	ditto	5YR 5/6
SE-82	17-22	73 km east of Richard-Toll	7.5YR6/4
SE-83	75-80	ditto	7.5YR6/4
SE-84	120-125	ditto	7.5YR6/4
SE-85	4-10	ditto	9YR 6/4

Methods of Grain-Size Analysis

All samples were taken for grain-size distribution by means of standard sieves. Calculations of the results were performed by using a package of menu-driven Polypascal computer programs for handling grouped observations data. This package is designed for use on a PC computer. Two of the programs solve the numerical problem of determining the estimates of the four main parameters of the log-hyperbolic distribution and their derivatives. The hyperbolic distribution is limited between the normal distribution and the skewed symmetrical Laplace distribution. Therefore it

is impossible to get a log-hyperbolic distribution for bi-modal sands. The package also contains a program for determining the mean, sorting, skewness and kurtosis according to the standard moments. Table 6 shows the four moment statistics and the mode (v) as calculated by the log-hyperbolic distribution. It was not possible to calculate the mode (n) in all samples because of having distribution behind the limit of the hyperbolic distribution.

Table 6: Results of the calculations of the standard moment statistics and the mode (v) according to the log-hyperbolic distribution.

Sample #	χ mean	Sd sorting	Sk skew-ness	Ku kurto-sis	Md median	v mode
1	0.069	0.734	-1.931	2 858	0 083	0.087
2	0.117	0.429	0.364	0.539	0.116	0111
3	0.085	0.411	2 028	6.923	0.080	0.073
4	0.124	0.538	0.432	0.381	0.124	0.155
5	0.736	0.564	-2.096	4.11	0.861	1.043
6	0.131	0 303	1.926	10 167	0.126	0.121
7	0.142	0.363	-0.251	1.092	0.150	0.158
8	0.146	0.281	0.159	1.020	0.149	0.145
9	0.172	0 738	1.328	1.405	0.151	0.130
10	0.283	0.396	-2.02	4.201	0 320	0.367
11	0.144	0.517	0 939	1.865	0.143	0.148
12	0.161	0 426	0.298	1.719	0.166	0.181
13	0.157	0.282	-1.679	14.899	0 159	0.157
14	0.379	0.796	-3.405	12.639	0.470	
15	0.158	0.423	-2.403	16.127	0.159	0.156
17	0.142	0.597	-2.49 ,	10.341	0.152	0.155
18	0.157	0 678	-0.913	3 254	0.160	0.161
19	0.151	0.733	-1.658	4.597	0.164	0.187
20	0.198	0.745	-1.494	3.615	0 241	0.293
21	0.162	0.775	-0.518	-0 146	0.168	0.163
22	0.146	0.498	0.561	-0.184	0.140	0.157

22b	0.181	0.555	-0.131	-0.991	0.184	0.312
24	0.190	0 549	0.169	-0.977	0.200	0.305
25	0.190	0.573	-0.166	-1.028	0.210	0 320
26	0.193	0.583	-0.158	-1.015	0.212	0 361
27	0.196	0.632	-0.172	-1.180	0 218	0.381
28	0.173	0.520	-0.061	-0.813	0.168	0 308
29	0.193	0 450	-0.175	-0.107	0 194	0.193
30	0.175	0 512	-0.035	-0 978	0.170	0.241
31	0 223	0.634	-0.188	-1.119	0 249	0.383
33	0.165	0 428	0.147	-0.156	0.163	0.171
34	0.170	0.406	0.110	-0.363	0.165	0 169
35	0.187	0.478	-0.174	-0 729	0.179	0 214
37	0.178	0.534	0 214	-0 481	0.169	0.181
40	0.171	0.390	-0.110	-0.213	0.168	0.164
41	0 175	0.403	-0.002	-0.443	0.170	
42	0.164	0 397	0 251	-0 379	0.158	0.160
43	0.156	0 688	0 909	-0.298	0.124	0.096
43b	0.169	0.776	0.644	-1.060	0.124	
44	0.159	0.730	0.806	-0.618	0.128	
45	0.182	0.682	0.604	-0.694	0.155	0.136
46	0.187	0 727	0.595	-0.954	0.154	0.088
47	0.160	0.649	0 921	-0 119	0.130	0.114
49	0.176	0.722	0.744	-0.805	0.142	0.096
58	0.164	0.686	0 647	-0.707	0.140	
59	0.188	0.727	0 372	-1.174	0.159	
61	0.162	0.726	0.477	-0.981	0.144	
62	0.172	0.767	0.335	-1.294	0 152	
63	0.154	0.686	0 580	-0.820	0.136	

64	0.173	0.731	0.398	-1.124	0.151	
65	0.180	0.740	0.326	-1.168	0.159	
66	0.177	0.736	0.402	-1.132	0 157	
67	0.204	0 718	0 214	-1.205	0.175	
68	0.188	0.758	0.198	-1.36	0.164	
69	0.194	0.692	0.175	-1.176	0.173	
70	0 179	0.650	0.38	-0.952	0.160	
71	0.172	0 769	0 509	-1.194	0.133	
72	0.180	0.764	0.466	-1 204	0.150	
73	0.164	0 672	0 296	-0.975	0.157	
74	0.206	0.756	0.234	-1 343	0.171	
75	0.174	0.759	0 508	-1.117	0.145	
76	0.186	0 735	0.415	-1.139	0.157	
77	0.148	0.305	0.348	2.436	0.152	0.161
78	0.147	0.309	0.234	1.762	0 152	0.161
79	0.147	0.263	-0.009	0.906	0.152	
80	0.142	0.280	-0.046	0.682	0.147	
81	0.148	0.265	-0.266	0.926	0.155	
82	0.207	0.581	-0.030	-0.599	0.209	
83	0.219	0.676	-0.218	-0.877	0.233	
84	0.223	0.654	-0.166	-0.855	0.241	
85	0.216	0.607	-0.202	-0.76	0.231	

Discussion

Normal distribution will show identical or near identical mean and mode. The correlation between the mean and mode (R=0.71) shows that in most cases there is a great difference between the two variables, which indicates a distribution different from typical active dune sand (Figure 9). It is obvious that above 135 µm, the mode is greater, in most cases, than the mean. This is typical for the bi-modal sand that is skewed toward the

coarse fractions. For that reason, the skewness is negative in those cases. Sand dunes, active or stabilized, are usually characterized by uni-modal distribution where the mode and the mean is between 250-125 μm (2-3ø)

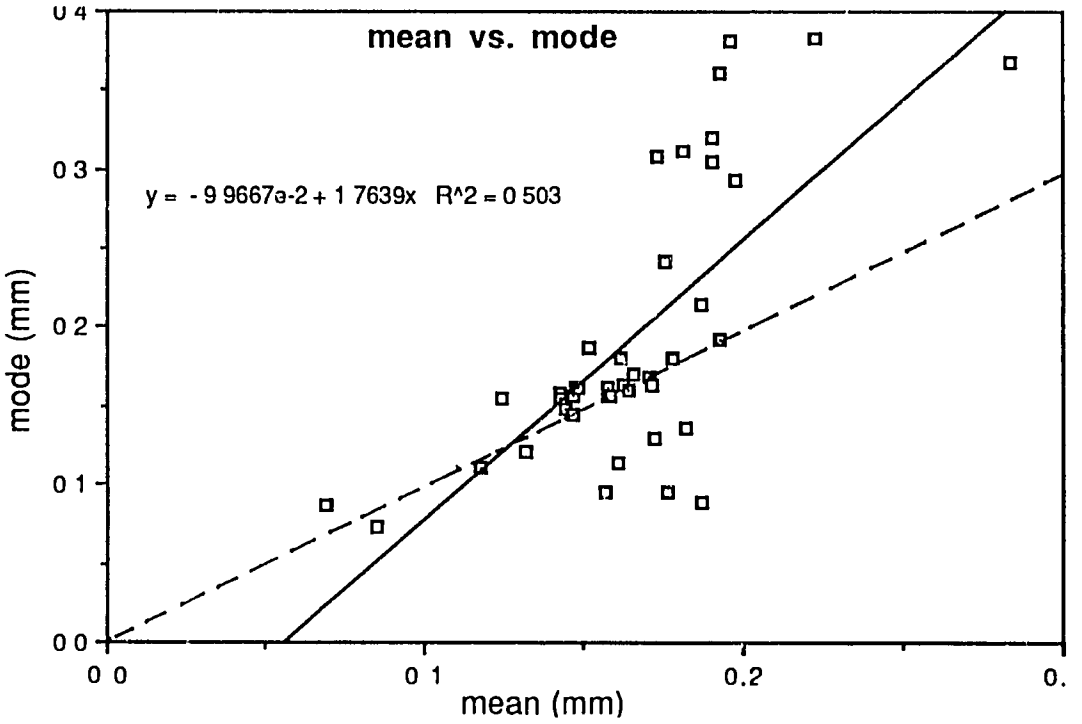

Figure 9: The correlation between mean (χ) and mode (ν). The dash line is the mean=mode line.

In northern Senegal the active saltating sand is in the range of 149-177 μm (2.5-2.84ø) However, there are sands where mean and mode are less than 100μm, such as samples 1 and 3 (Figure 10), which are of saltating sand of small dunes, and samples 2 and 4, that were taken from the small linear dune that was formed during the storm. It seems that this very fine sand and silt was transported in modified saltation from a local source of fluvial material. Samples that were taken from the slip face of an active seif dune shows a bi-modal distribution with one dominant mode (Figure 11), where the main mode is still smaller than the grain-size expected for active saltating sand and the second mode is in the range of saltating sand. The source of this sand is from a nearby ancient linear dune that is eroded. Figure 12 shows the grain-size distribution of the ancient linear dune. It is obvious that these two samples have the same distribution with the same mean and mode.

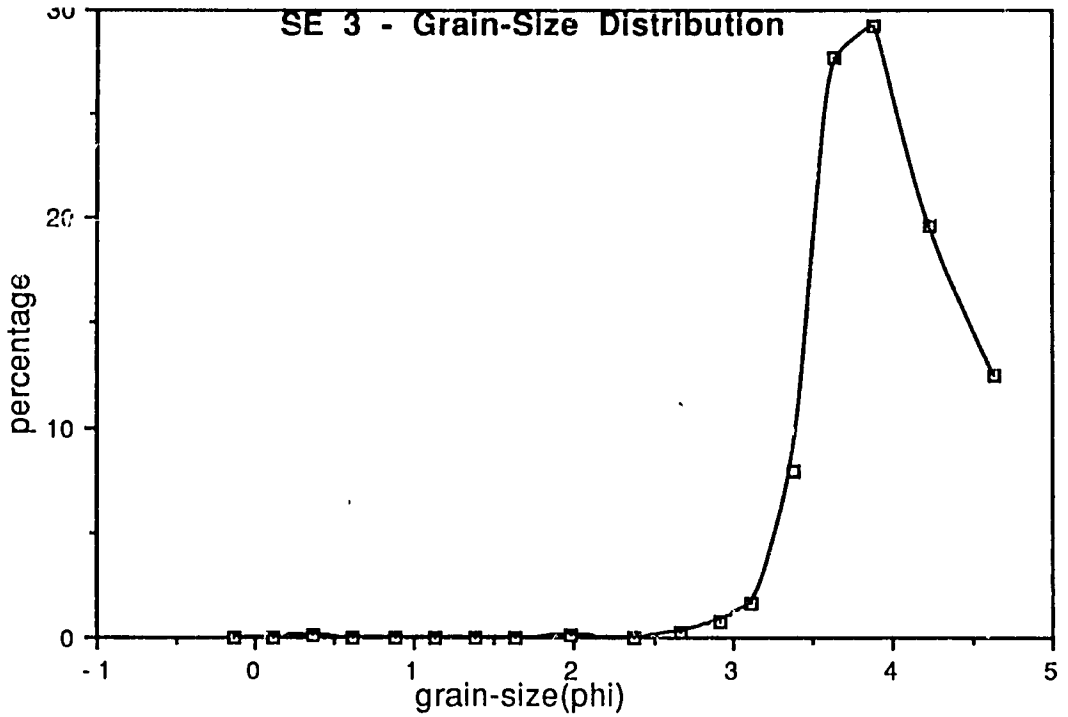

Figure 10: The distribution of sample #3 that shows mean and mode in the very fine sand and silt fractions.

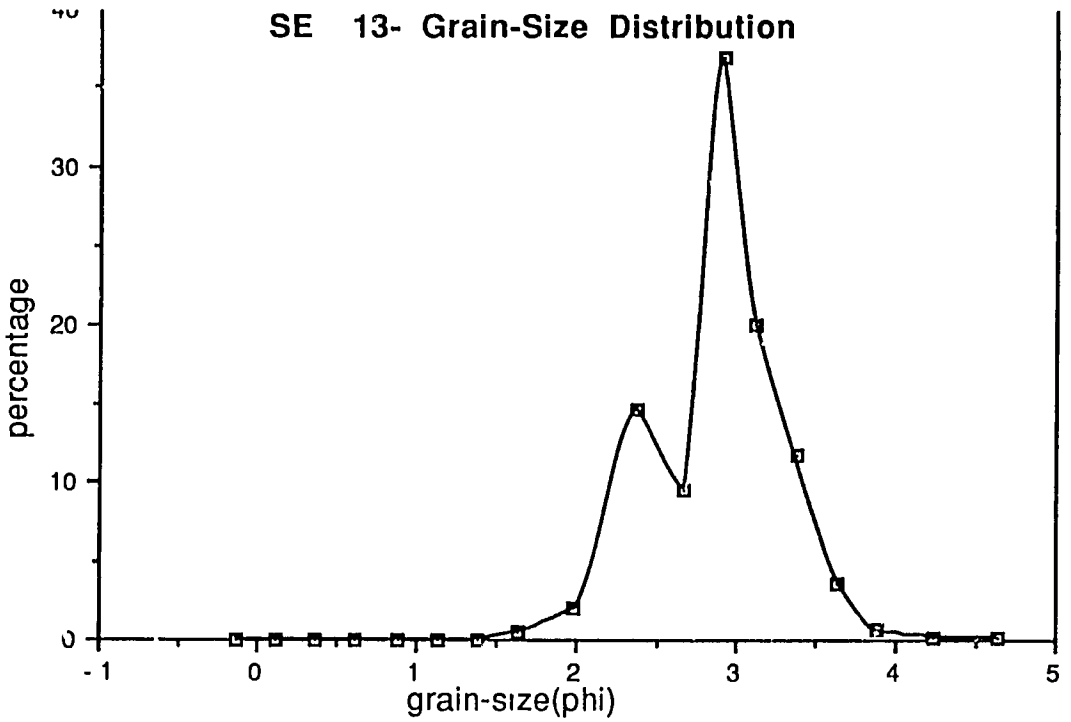

Figure 11: The grain-size distribution of sand sample taken from the slip-face of an active seif dune.

Samples that were taken from an active slip-face of seif dune eastward to the previous dunes show a coarser mode of 0.161 mm in a typical uni-modal sand. An example is the distribution of sample SE-79 (Figure 13). SE-79 is slightly bi-modal with a second minor mode in the 3-3.25Ø range,

which is at the upper part of the modified saltation range. This indicates a contribution of particles moved by modified saltation, probably during the Harmattan period. Samples SE-77 and SE-78 were taken from an ancient linear dune at two depths: 4-9 cm and 23-28 cm, respectively. They were also uni-modal in their distribution, with a small amount of aggregates around 2Ø (Figures 14 & 15).

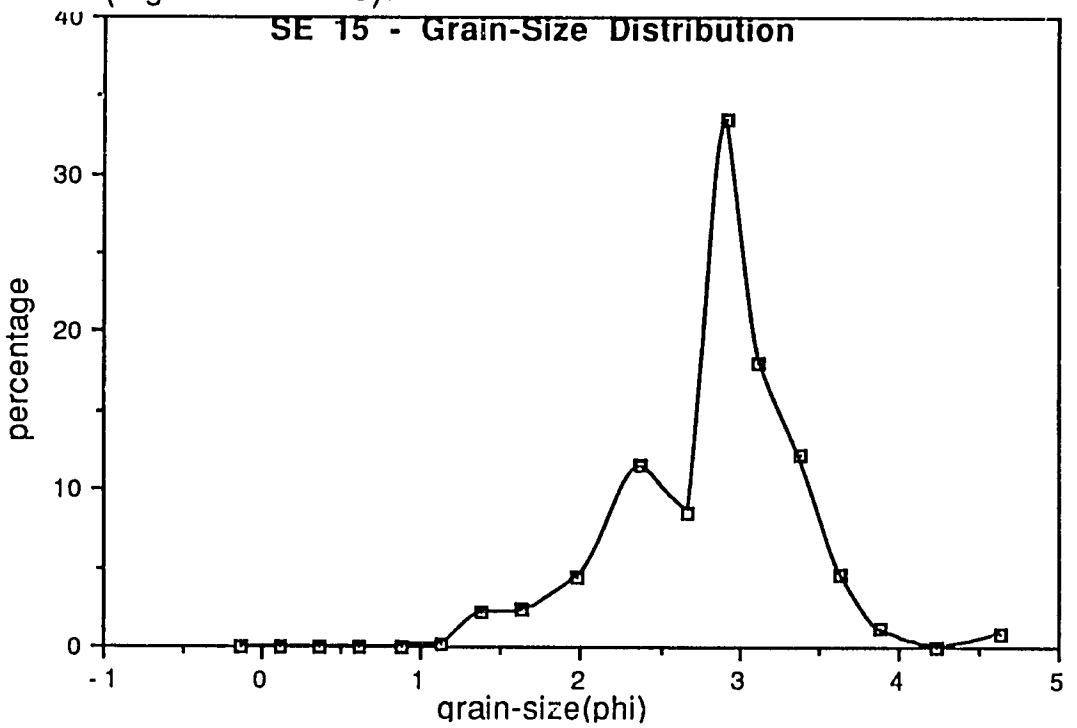

Figure 12: The grain-size distribution of ancient stabilized linear dune that was recently eroded by the wind.

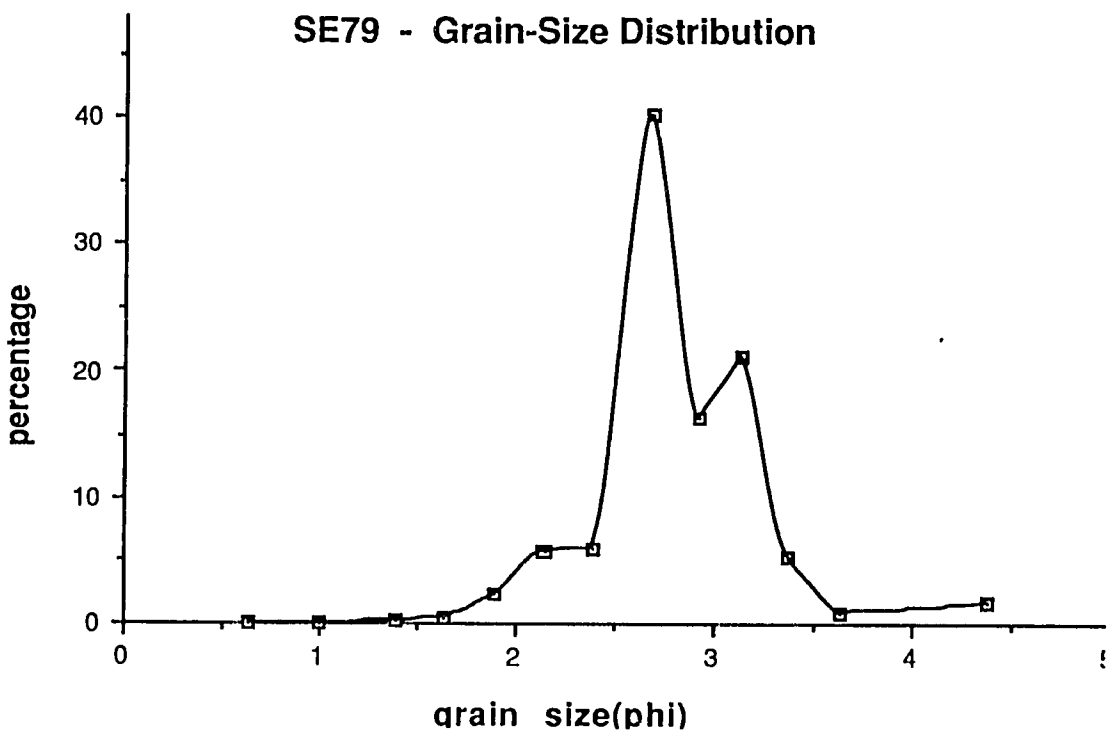

Figure13: Grain-size distribution of slip-face sand of an active seif dune. Note that in this sample the main mode is the secondary mode

in Figure 11, while the main mode there is secondary here.

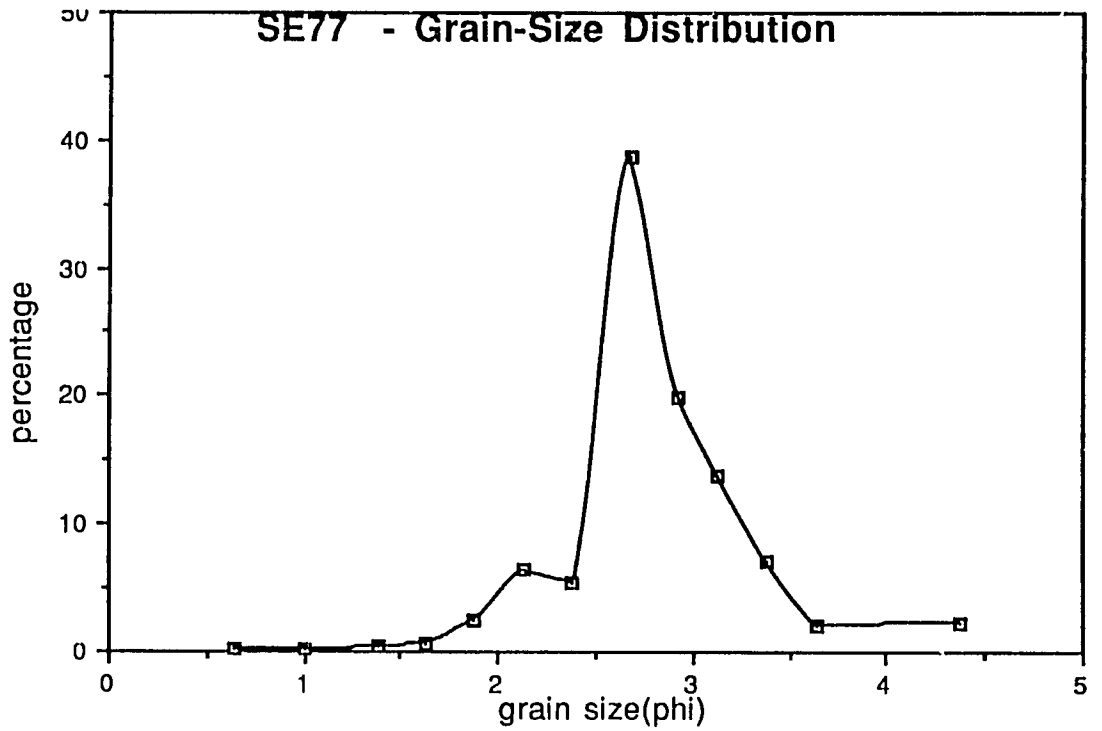

Figure 14: The grain-size distribution of an ancient fixed dune. Note the similarity between this distribution and the one of Figure 13, which is of an active seif dune whose sand was eroded from the ancient fixed dune.

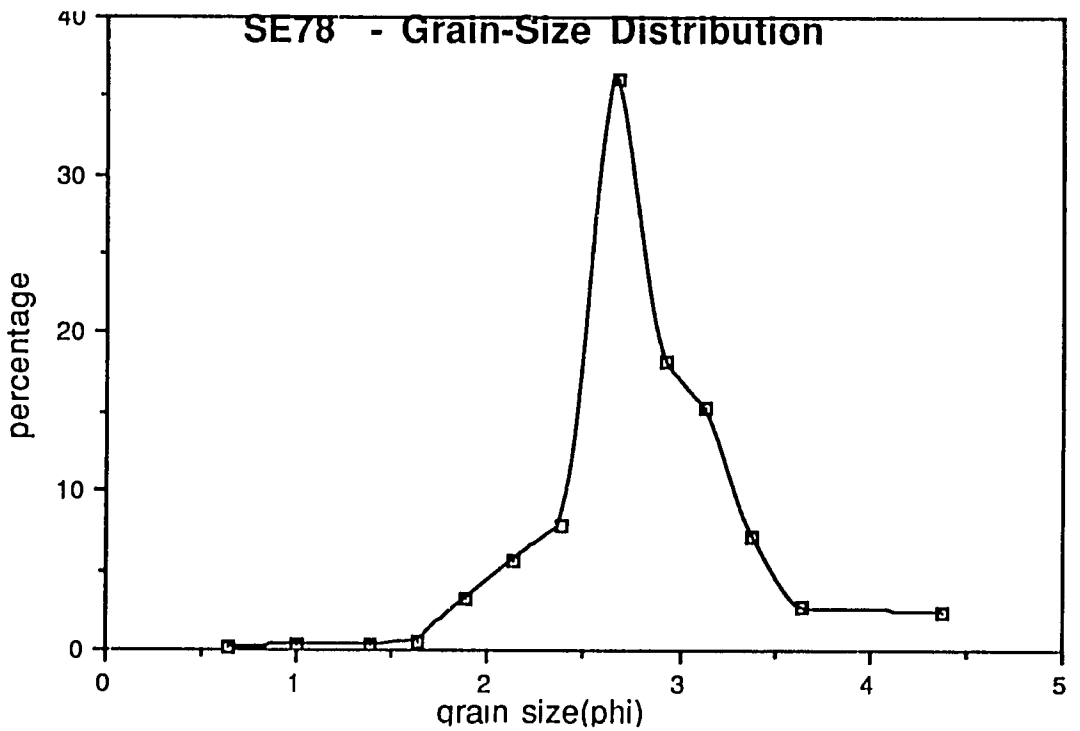

Figure 15: The grain-size distribution of an ancient fixed dune. Note that this distribution is not bi-modal, as was the one of Figure 14. It was taken at greater depth.

Most of the sand samples in northern Senegal indicate that the eolian sand sheets there are either bi-modal or in most cases multi-modal. However, one of the modes is always in the saltating sand range for northern Senegal, which is in the 2.5-2.84ø range. This property characterizes all the sand sheets of Senegal. However, several types of grain-size distributions were discerned.

An example for the sand sheets' grain-size distribution are samples 22 to 37, which were taken at different depths of an ancient linear dune with a north-east to south-west orientation. The dune is not active, but has been deeply eroded south of the road, apparently by water. The inner part of the dune is exposed, exhibiting a composite profile to a depth of about 10 meters below the dune surface Figure 16 shows the grain-size distribution of two samples, SE 22b and SE 37. The first one was taken from a depth of 50-55 cm below the surface and the second sample from a depth 935-940 cm. There is not much change in the grain-size distribution with depth. The mode is changed with greater values than the mean with depth. Figure 17 shows the changes in mode and mean from the surface to 10 meters depth. The changes in the mode resultes from small changes in the proportion of a fraction that has small effect on the mean. There is a good correlation between the mean and mode (R=0.721).

The poly-modal distribution is very obvious and identical in the two samples (Figure 16) One mode is in the very fine sand fraction, as it is with sample SE 13 (Figure 11); the other mode is in the fine sand fraction, which is the typical grain-size moved most easily in saltation, as it is in sample 78 (Figure 15). The third mode is in the medium sand fraction Inspection of the grains by binocular shows that the medium and coarse modes of the sand samples are not aggregates, but are clearly discrete grains.

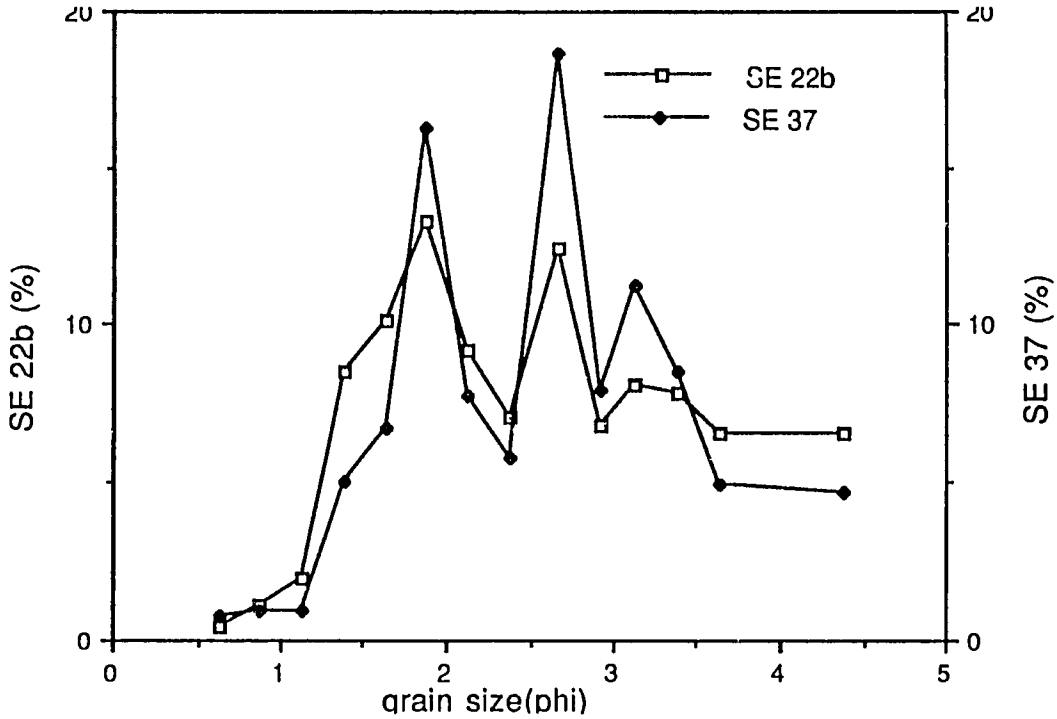

Figure 16: Grain-size distribution of two samples taken from an ancient fixed linear dune at two different depths.

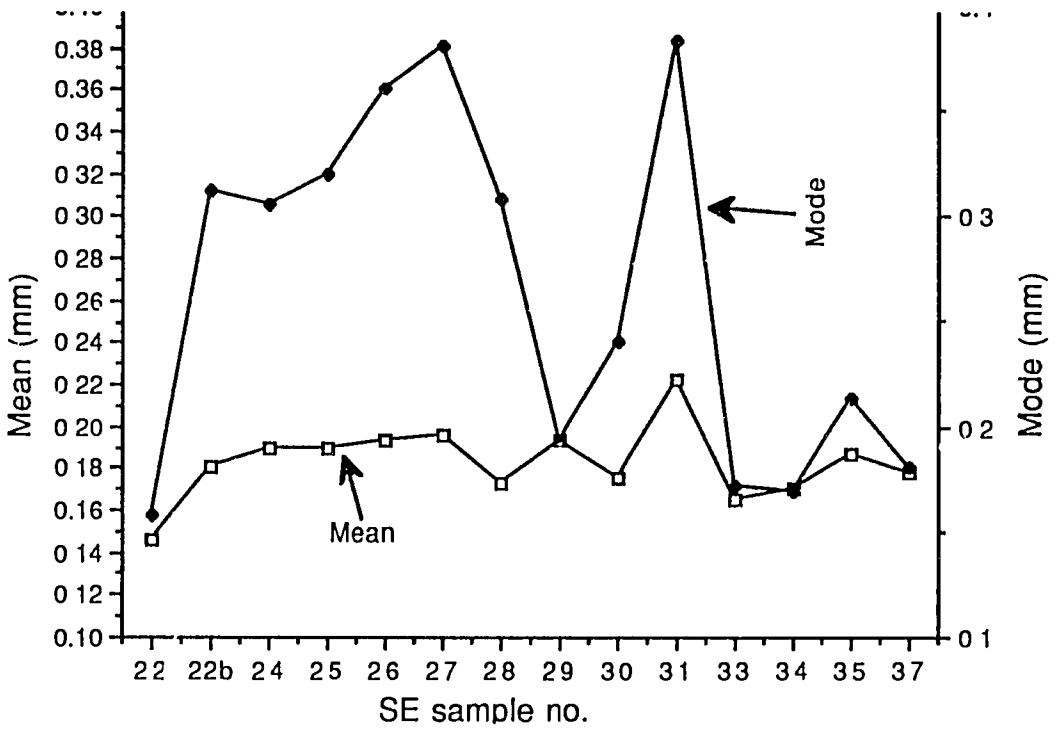

Figure 17: Changes in mode and mean of samples taken from the surface to a depth of 10 metres

Most of the samples taken in the field have this poly-modal distribution with different proportions of the the three modes. Some of them have four modes, the smallest one in the silt fraction, then very fine sand, fine sand, and medium (coarse) sand (Figure 18).

Samples 43 to 49 were taken 1 km east of Ndioum in an area characterized by flat, slightly undulated stable sand sheet. Samples were taken from surface and the crust to depth of 345 cm. A brown soil has developed in the upper part of the profile.

According to Figures 18 and 19, there is no difference in the grain-size distribution of the sand sheet from the crust to a depth of 350 cm This fact indicates that, in spite of the pedological processes, the sand sheet has been through, the grain-size has barely changed.

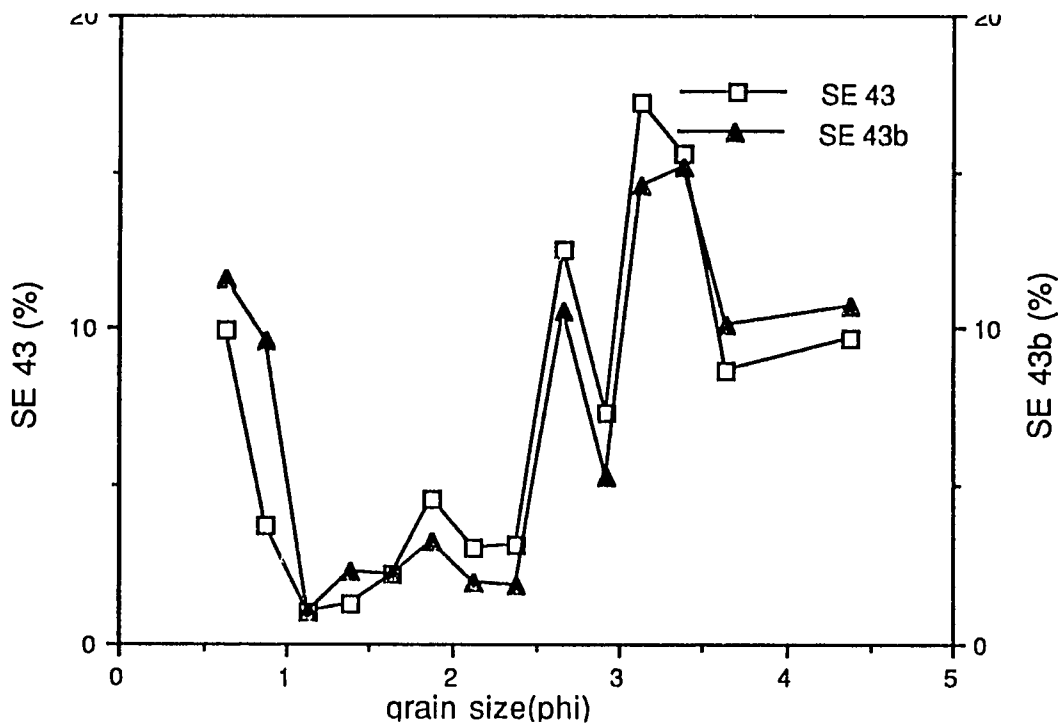

Figure 18: Grain-size distribution of two samples taken from a sand sheet upper part soil (SE 43) and the surface crust (SE 43b).

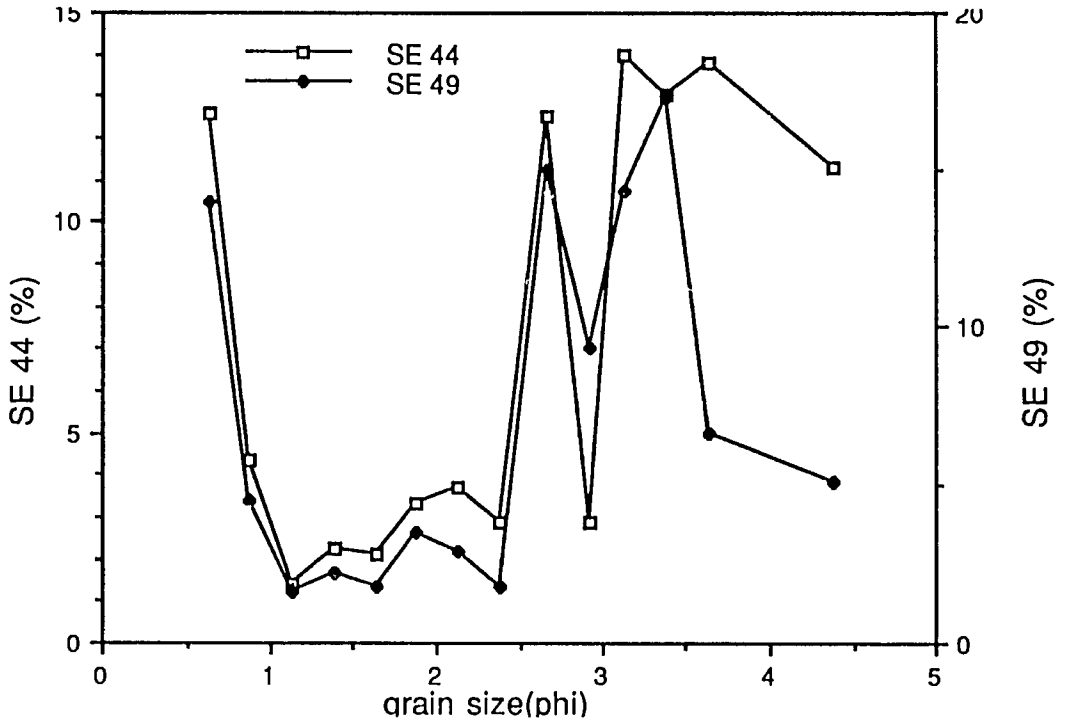

Figure 19: Grain-size distribution of two samples taken from a sand sheet at two depths: SE 44 at 5-8 cm and SE 49 at 340-345 cm.

In conclusion, most of the sand sheets of northern Senegal are composed of poly-modal sand that has a distribution that is not known from other areas of the world. It seems that it is composed of several populations that are the result of processes of erosion and deposition. The mode between 2 and 3ø is known as the mode of the saltating sand under the present wind regime. Such sand can accumulate when the area is vegetated. When the vegetation is destroyed and much stronger winds blow, the erosion of the most easily transported grains in the range of 1.0 to 2.5ø will bring about a coarse mode in the range >1 0ø Long periods of wind just above the threshold, such as the Harmattan winds, will only carry grains that are < 3.0ø. This will create the third important mode of very-fine sand and silt.

Chemical and Mineralogical Analyses of the Sand Samples

Methods

The Senegal sand samples have been analyzed as follows:

1. Bulk sediment X-ray fluorescence spectometry analysis to determine major element composition.

2. Bulk sediment X-ray powder diffraction analysis to determine major mineral composition.

3. Determination of elements extractable after boiling in 50% HCl for 20 minutes; analysis by inductively coupled plasma spectrometry (Fe, Mn, Ca, Mg, Al, Si) and atomic absorption spectrometer (Na, K). This provides a measure of the degree of reddening and an indication of the thickness and composition of clay coating development in the sands.

4. Determination of cold (i.e. 16°C) de-ionized water extractable ions (Cl-, SO_4, NO_3), determined by ion chromography Leaching is accomplished by placing each sub-sample in a test tube filled with 50 ml of de-ionized water and agitating it ultrasonically for 24 hours.

5 SEM examination of grain surface texture and X-ray microanalysis to determine the composition of individual grains and their coatings.

Since none of the samples showed visible reaction with 50% HCl, the carbonate content was not measured independently. No carbonate minerals were detected by XRD.

Table 7: SEM surface texture analysis

	SEM surface texture	XRD Mineralogy
SE 2	thick grain coatings Si, Al, Fe, Li, K	Q, KF, trace, Pf, K, Ch
SE 3	subangular grains, thick coatings	Q trace KF, PF
SE 4	thick coatings, fine grain aggregates, some CL cemented	Q, H trace KF
SE 5	clean grain surfaces , subrounded to subangular	Q

SE 7	subangular grains predominant, thin to moderately thick Fe-clay coatings	Q trace KF
SE 8	subangular to subrounded, mostly clean	Q
SE 9	subrounded to subangular, thin to moderately thick coatings	Q trace KF
SE 10	as above	Q trace PF
SE 11	thick grain coatings	Q trace KF
SE 12	subrounded grains predominant, thick to moderately thick coatings	Q trace KF, K, Ch
SE 13	subrounded subangular grains, thin coatings, Fe and clay restricted to pits	Q
SE 14	subrounded to rounded, mainly clean	Q
SE 15	subrounded to subangular	Q
SE 17	moderate to thick grain coatings, fine aggregates, some CL-cemented, diaton fragments	Q
SE 18	moderate to thick coatings, fine fungal hyphae	
SE 19	moderate to thick coatings, aggregates, clay pellets	Q
SE 20	as above	Q
SE 21	as above	Q

Table 8: X-ray diffraction results summary, bulk sediment X-ray diffraction. X major constituent; tr trace; - not detected.

Sample	Quartz	Plagioclase	Haematite	K-Fledspar
SE 22	X	-	-	tr
SE 22B	X	-	-	tr
SE 24	X	-	-	tr
SE 25	X	-	-	tr
SE 26	X	-	-	tr
SE 27	X	-	-	tr
SE 28	X	-	-	tr
SE 29	X	-	-	tr
SE 30	X	-	-	tr
SE 31	X	-	-	tr
SE 32	X	-	-	tr
SE 33	X	-	-	tr
SE 34	X	-	-	tr
SE 37	X	-	-	tr

SE 40	X	-	-	tr
SE 41	X	-	-	tr
SE 42	X	-	-	tr
SE 43	X	-	-	tr
SE 43B	X	-	tr	tr
SE 44	X	-	tr	tr
SE 45	X	-	tr	tr
SE 46	X	-	tr	tr
SE 47	X	-	-	tr
SE 49	X	-	tr	tr
SE 73	X		tr	tr
SE 74	X	tr	tr	tr
SE 75	X	-	-	tr
SE 76	X	-	-	tr

Table 9: Results of chemical extraction (ppm). Multiply by 14^{-4} for weight in percent.

	50% HCL extractable						De-ionized water extractable				
Sample	Fe	Mn	Ca	Mg	Al	Si	Na	K	Cl	SO_4	NO_3
SE 2	7216	133	570	1035	3685	2001	1743	363			
SE 3	8744	116	849	819	6435	2441	253	554			
SE 4A	9988	131	912	1373	6518	2947	2302	445			
SE 4B	6920	161	787	3148	4344	1893	2516	377			
SE 5	8477	29	246	125	1521	715	76	97			
SE 7	2903	26	592	219	1947	1535	90	130			
SE 8A	1864	25	149	88	790	785	57	95			
SE 8B	1967	25	156	107	1279	1045	85	113			
SE 9	4127	43	222	197	1825	1419	64	106			
SE 10	2908	37	283	249	2183	1700	80	163			
SE 11A	4237	29	228	175	2303	1704	90	127			
SE 11B	4077	26	182	169	2149	1564	79	123			
SE 12	5514	28	158	186	2727	1707	58	114			
SE 13	1576	11	216	93	762	704	58	77			
SE 14A	1072	8	109	60	758	378	68	73			
SE 14B	1533	9	117	68	647	579	48	48			
SE 15	2349	30	230	181	1785	1103	67	175			
SE 17	3107	43	542	416	2808	1704	152	279			
SE 18A	2325	35	448	297	1709	1588	96	238			
SE 18B	2255	34	583	275	1701	1934	95	200			
SE 19	2971	52	390	248	2387	1952	71	183			
SE 20	1918	37	697	256	1218	1131	67	131			
SE 21A	4936	43	478	222	3006	2218	58	104			
SE 21B	5635	57	403	293	4773	2755	55	132			
SE 22	2928	43	709	247	2513	2142	722	255	3428	672	1192
SE 22B	2615	45	638	214	4882	1968	596	198	4268	1069	655
SE 24	2722	29	579	172	1722	1867	581	119	235	605	673

SE 25	2447	19	526	148	1990	1782	640	103	3277	3213	685
SE 26	2709	25	680	131	1733	1368	710	108	739	231	2550
SE 27	1917	9	532	109	1473	1356	589	77	4729	735	1515
SE 28	2595	16	654	149	2110	1379	687	156	909	5763	921
SE 29	619	14	558	136	2096	1963	619	136	3430	603	846
SE 30	2175	11	647	136	1923	1895	620	127	6246	3862	1847
SE 31	1959	10	550	114	1145	1190	637	95	2080	1210	1239
SE 32	2093	7	387	121	1897	2011	443	103	837	384	643
SE 33	2346	18	568	141	2147	1291	716	156	5859	1145	11962
SE 34	2047	11	515	123	1850	1446	630	121	342	110	592
SE 37	4248	31	1831	314	3252	1807	737	235	3666	7708	1044
SE 40	3708	58	654	260	3038	1550	521	301	1420	420	984
SE 41	3372	33	570	189	2563	2081	447	207	30736	3265	1547
SE 42	2911	26	676	182	2452	1974	614	174	766	220	672
SE 43	6178	113	762	362	4019	3000	654	437	391	110	770
SE 43B	5389	87	712	267	2339	2081	591	282	1453	429	3937
SE 44	6137	82	477	223	2515	2052	416	260	65288	14354	1529
SE 45	6883	98	861	352	4489	2539	766	460	15781	2218	749
SE 46	9497	98	696	350	5515	2589	580	411	379	<20	616
SE 47	7595	100	763	317	5291	3102	603	321	1231	4224	1068
SE 49	5872	66	832	255	4454	2649	476	271	2329	636	940
SE 73	5015	49	858	423	2251	2048	524	323	1248	510	1000
SE 74	11208	85	757	274	3723	2644	513	352	671	941	637
SE 75	19745	63	1722	261	2063	1742	631	167	810	106	629
SE 76	15022	63	1018	276	3159	2687	736	326	441	226	620

Table 10: Whole-Rock XRF Major Element Data

Sample	Na_2O	MgO	Al_2O_3	SiO_2	P_2O_5	K_2O
GSP-1	2.46	0.96	15.1	67.69	0.3	5.67
DRN	2.64	4.4	17.6	53.87	0.25	1.7
G24.45	0.81	15.4	68.64	0.16	4.67	
SE 2	0.56	0.28	3.92	89.17	0.03	0.53
SE 3	0.01	0.15	3.91	90.15	0.15	0.74
SE 4	0 87	0.34	5.09	84.8	0.05	0.61
SE 5	0.01	0.01	0.17	94.65	0.02	0.02
SE 7	0.01	0.01	1.99	95.11	0.03	0.26
SE 8	0.01	0.01	0.84	96.84	0.03	0.07
SE 9	0.04	0.02	2.18	91.9	0.08	0.16
SE 10	0.01	0.01	1.5	96.07	0.01	0.14
SE 11	0.15	0.01	1.98	94.09	0.05	0.48
SE 12	0.01	0.01	3.7	92.06	0.01	0.15
SE 13	0.01	0.01	0.69	98.71	0.02	0.05
SE 14	0.01	0.01	0.31	98.9	0 01	0.01
SE 15	0.01	0.01	0.76	97.02	0.06	0.17
SE 17	0.01	0.04	1.22	95.58	0.03	0.16
SE 18	0.01	0.01	0.93	95.45	0.03	0.13
SE 19	0.01	0.01	1.5	94.99	0.05	0.11
SE 20	0.01	0.24	0.99	95.87	0.42	0.13
SE 21	0.01	0.06	2.59	92.42	0.12	0.2
SE 22	-0.45	-0.03	0.86	98.43	0	0.06

SE 22B	-0.46	-0.02	0.78	98.39	0	0.04
SE 24	-0.46	-0.03	0.71	98.95	-0.01	0.02
SE 25	-0.47	-0.03	0.68	98.93	-0.01	0.01
SE 26	-0.47	-0.05	0.45	99.52	-0.01	-0.01
SE 27	-0.46	-0.05	0.59	99.49	-0.01	0
SE 28	-0.44	-0.05	0.68	98.8	-0.01	0
SE 29	-0.46	-0.04	0.61	98.9	-0.01	-0.01
SE 30	-0.48	-0.03	0.73	98.52	-0.01	0.01
SE 31	-0.46	-0.03	0.51	99.46	0	0
SE 32	-0.46	-0.05	0.63	99.5	-0.01	0.01
SE 33	-0.45	-0.3	0.59	99.38	-0.01	-0.01
SE 34	-0.48	-0.04	0.57	99.5	-0.01	-0.01
SE 37	-0.46	-0.01	1.28	97.86	-0.01	0.05
SE 40	-0.44	0.02	1.33	97.26	0.02	0.11
SE 41	-0.46	-0.02	1.01	98.02	0.02	0.06
SE 42	-0.46	-0.03	0.81	98.21	0	0.07
SE 43	-0.44	0.01	1.87	95.47	0.01	0.19
SE 43B	-0.42	0.01	1.63	96.06	0.01	0.21
SE 44	-0.44	0.00	1.43	97.07	0.01	0.15
SE 45	-0.43	0.04	3.16	93.83	0.01	0.2
SE 46	-0.36	0.03	2.65	94.44	0.01	0.17
SE 47	-0.46	0.02	2.65	94.07	0	0.15
SE 49	-0.44	0.01	2.64	94.61	0.01	0.17
SE 73	-0.33	0.07	1.47	95.89	0.02	0.26
SE 74	-0.43	0	2.29	94.26	0.01	0.19
SE 75	-0.41	0.03	1.35	94.57	0.02	0.17
SE 76	-0.44	0	1.76	95.85	0.05	0.17

CaO %	TIO_2 %	MnO %	Fe_2O_3 %	LOI %	TOTAL %	
SE 2	0.09	0.43	0.03	1.86	3.42	100.31
SE 3	0.1	0.42	0.21	1.69	2.52	99.67
SE 4	0.15	0.41	0.03	2.5	4.94	99.78
SE 5	0.01	0.1	0.02	3.11	1.38	100.21
SE 7	0.03	0.26	0.01	0.71	1.55	99.86
SE 8	0.01	0.16	0.01	0.43	1.16	99.24
SE 9	0.01	0.27	0.02	1.99	1.72	98.37
SE 10	0.01	0.21	0.06	0.59	1.07	99.37
SE 11	0.01	0.32	0.01	1.02	1.65	99.73
SE 12	0.01	0.28	0.01	1.27	2.17	99.41
SE 13	0.01	0.15	0.01	0.39	0.71	100.42
SE 14	0.01	0.04	0.01	0.26	0.44	99.65
SE 15	0.01	0.17	0.01	0.45	0.96	99.49
SE 17	0.12	0.21	0.01	0.68	1.47	99.40
SE 18	0.03	0.20	0.01	0.47	2.14	99.22

SE 19	0.01	0.28	0 01	0.63	1.71	99.08
SE 20	0.04	0.29	0.01	0.49	1.50	99.33
SE 21	0.05	0.37	0.01	1.31	2.08	99.19
GSP-1	2.034	0.706	0.042	4.323	0.700	99.985
DRN	6.906	1.097	0.216	9.674	2.350	100.719
G22.065	0.509	0.035	2.655	0.580	99.958	
SE 22	0.042	0.173	0.009	0.554	0.000	99.644
SE 22B	0.044	0.185	0.011	0.566	0.000	99.535
SE 24	0.036	0.115	0.008	0.534	0.000	99.884
SE 25	0.027	0.174	0.007	0.499	0.000	99.809
SE 26	0.022	0.124	0.005	0.427	0.000	100.011
SE 27	0.021	0.194	0.007	0.483	0.000	100.252
SE 28	0.022	0.177	0.005	0.491	0.000	99.685
SE 29	0.025	0.144	0.014	0.469	0.000	99.652
SE 30	0.035	0.187	0.005	0.496	0.000	99.461
SE 31	0.024	0.150	0.005	0.439	0.000	100.089
SE 32	0.019	0.106	0.004	0.435	0.000	100.719
SE 33	0.028	0.131	0.005	0.434	0.000	100.071
SE 34	0.024	0.129	0.005	0.434	0.000	100.126
SE 37	0.155	0.152	0.008	0.798	0.000	99.820
SE 40	0.059	0.166	0.013	0.778	0.000	99.321
SE 41	0.044	0.139	0.009	0.620	0.000	99.440
SE 42	0.035	0.143	0.007	0.562	0.000	99.351
SE 43	0.059	0.331	0.021	1.106	0.000	99.627
SE 43B	0.075	0.353	0.019	1.053	0.000	98.627
SE 44	0.053	0.292	0.019	1.407	0.000	98.730
SE 45	0.069	0.312	0.019	1.590	0.000	99.580
SE 46	0.062	0.292	0.017	1.407	0.000	98.730
SE 47	0.064	0.278	0.028	1.404	0.000	98.202
SE 49	0.083	0.286	0.015	1.359	0.000	98.744
SE 73	0.138	0.249	0.013	1.084	0.000	98.871
SE 74	0.062	0.289	0.018	2.093	0.000	98.788
SE 75	0.202	0.231	0.014	1.301	0.000	97.491
SE 76	0.112	0.239	0.015	1.579	0.000	99.344

N.B. Total iron reported as Fe_2O_3.

LOI - Loss on ignition at 1000°C (includes structural water, and oxygen from organic matter, carbonates and sulphates; some carbon and sulphur also lost).

Negative values are below limits of detection.

Results

Results are shown in Tables 8, 9, 10 and in . The X-ray diffraction results of grain surface coating are shown in Appendix 3. The SEM photographs showing the grains are in Appendix 4. All of the samples are dominated by quartz sand with very minor amounts (less than 5%) of feldspar and heavy minerals which are found mostly in some of the samples taken northeast of Richard Toll (SE 43-SE 76). Hematite and/or geothite are the only other crystalline minerals detectable by whole rock XRD. They are present as part of the grain coatings, which are mostly composed of amorphous alumino-silicate material. Carbonate is virtually absent.

Samples SE 2, 3 and 4 are all very rich in HCl-extractable Fe, Mn, Ca, Mg, Si, Al, Na, and K. This reflects a high content of clay minerals, iron oxides (including crystalline haematite), and soluble salts (especially in the dune crust sample). This probably reflects airborne dust additions, but the high Mn content is suggestive of partial derivation from laterite outcrops, and Na and K salts may be derived from saline clay deposits in the Senegal River valley.

All of the old linear dune sands are reddened and have Fe/clay rich grain coatings. The surface crusts are especially rich in these constituents and soluble salts, which helps to bind the grains together.

The seif dune and megaripple sands which appear to be the result of reworking of the older linear dunes contain much less iron and clay. They have relatively clean surface textures, with Fe oxides and clay restricted mainly to surface pits.

The samples from the linear dune section (SE 22-SE 37) are interpreted as follows:

SE 22 represents a relatively recent influx of brown-yellow sand which has covered the surface of a stabilized dune containing a soil profile in the upper 1.5 m. The palaeosol contains slightly higher levels of extractable Fe, Ca, Mg, Si, Al, Na, K, Cl-, SO_4 and NO_3 than the underlying sand, reflecting the presence of organic matter and biogenic enrichment. The grains show moderately developed coatings, including recognizable organic remains. Between 1.5 and 6.65 m in depth, the sands are relatively clean, with small amounts of aluminosilicate material and iron oxides concentrated in pits on the grain surfaces; these are probably detrital features. The basal sands in this profile have been affected by groundwater movement, hence the gleying. The reddish-orange sand SE 37 is notably enriched in extractable Fe, Mn, Ca, Mg, Al, Si, Na, Cl, K, SO_4 and NO_3.

SEM revealed the presence of thick but somewhat patchy alumino-silicate - Fe oxide cements/coatings. Since the field descriptions and the grain-size data give no indication that it is a distinct lithological unit, groundwater enrichment of this sand appears most likely.

The sequence of samples SE 40-SE 42 represent brown soil horizon sands overlying less modified yellow-brown sand sheet deposits. Total amounts of extractable Fe, Mn, etc. are lower than in the other sand sheet deposits described below, suggesting a younger age.

The entire 3.45 m thick sand sheet sequence SE 43-SE 49 contains high levels of extractable Fe, Mn, Mg, Al, and Si, although the more mobile elements Na, Ca, and K are not notably enriched. Salts are again concentrated between 8 and 115 cm below the surface. The grains are characterized by relatively thick alumino-silicate-Fe oxide coatings. This sequence may be of some considerable age; i.e., late Pleistocene.

The thin pale orange 'loess' (SE 73) covering the sand sheet sequence (SE 74-SE 76) contains quite high amounts of extractable Fe, Mn, etc., but much of this is probably inherited from the source sediments and the 'loess' itself may be quite young (Holocene?). The underlying sand sheet deposit (SE 74) is a dark brownish orange, has higher extractable Fe, Mn, etc., and must be considerably older. It has been partially modified by syn- or post-depositional pedogenesis. SE 75 is brown in color and represents a palaeosol A horizon developed in an older sand sheet unit. It contains exceptionally high levels of extractable Fe. SE 76 represents part of the same depositional unit which has been less enriched in Fe, but more enriched in Si/Al during pedogenesis. We would anticipate a late Pleistocene age for SE 74-SE 76.

The results show the very homogeneous character of sedimentation for this ancient sandsea; e.g., bimodal distribution and uncomplete eolization of the sand grains, presence of ubiquitous heavy minerals, a fine fraction of clay composed out of illite and kaolinite, and Fe clay.

DATING

Radiocarbon dating of charcoal samples from a fossil linear dune in northern Senegal

Dune formation is episodic, with periods of eolian activity alternating with periods of dune stabilization, weathering, and pedogenesis. Data are insufficient to decide whether the discrete dune emplacement events, as observed in Northern Senegal, are random events related to local sediment budget changes, or whether these are nonrandom events associated with climatic changes, cycles of storminess, or man's impact on the environment. Such hypotheses might be tested by dating the dune sequences at several sites.

There are problems in dating dune sand, particularly that of northern Senegal. Two main methods are used to date dune sand: radiocarbon dating and thermoluminescence (TL), each of which has advantages and disadvantages. We were able to use the radiocarbon method, which is less problamatic than the thermoluminescence method, in spite of the fact that radiocarbon is difficult in subtropical environments, since organic matter and shells in freely-drained quartz dunes decay or dissolve relatively rapidly.

GEOMORPHIC DESCRIPTION OF THE AREA WHERE SAND WAS DATED

The area is characterized by various ancient linear dunes, usually stabilized, situated about 15 km east of the Atlantic coast and immediately south of the Senegal river floodplain. The general orientation of the linear dunes in this area is from north-east to south-west.

Site IV was chosen for investigation because two active seif dunes were found on top of an ancient linear dune. The ancient dune is, in a rough estimation, approximately 800 m long, 80 m wide, and 10 m high. From its upper part, the floodplain of the Senegal river, including a large meander of the Lampsar river branch, can be seen to the north. The floodplain in fact constitutes the northern border of the linear dunes in this area.

The longest seif dune, approximately 100 m long, has formed on the top south-western part of the linear dune. On the day we visited the site (15.3.90), the Harmattan wind was blowing in sand from the east. The active slip face (SE- 13: sample of sand from the active slip face) on the western part of the seif dune ranges in height from about 1 to 3 m. The other seif dune is much smaller in size and is situated more to the north-east top of the same linear dune.

LAND USE TODAY

According to a local herdsman whom we encountered at the site, millet and cow peas are grown on the stable dunes and sand sheets in the region in the rainy season (June to October). According to the same herdsman, there is no moving sand during that time of the year.

MOVING SAND ON 15 MARCH 1990

On 15.3.90, moving sand was blown in with the Harmattan wind from the east, but its source has not yet been established. While part of the sand accumlated on the active seif dunes, much sand continued to move leeward from the seif dunes, forming active megaripples (SE 14: sample of coarse sand from the crest of these megaripples). The saltating sand causes active deflation of the surface of the linear dune, leeward of the seif dunes, in between them, as well as on other parts of them. (SE 15: sample of stratified sand from a profile at the upper part of the linear dune, exposed due to deflation).

Eventually the sand accumulates as a loose cover on the western leeward slope of the linear dune. Here it is sheltered from the eastern Harmattan wind and comes to rest, and does not appear to be moving further west, onto the next linear dune. The latter dune is stabilized with a dark crust and does not exhibit signs of active sand accumulation or erosion. (SE 17: surface sample with crust from the next [stable] linear dune).

CHARCOAL SAMPLES FOR RADIOCARBON DATING

The charcoal was collected from two adjacent spots, about 50 m apart, on the upper part of the ancient linear dune. This stretch of the linear dune, situated more or less in between the two seif dunes, is particularly affected by deflation. Many pottery sherds and some charcoal appear at the surface, exhumed as a result of sand laden winds which batter the surface of the ancient dune, dislodging sand and grains. The heavier pottery and charcoal pieces remain on the surface as a lag deposit. Many large mollusc shells, supposed to be of terrestrial origin, also appear at the surface, and these ought also to be dated by radiocarbon.

Charcoal samples and description:

Senegal-100	Charcoal amidst pottery sherds on deflated surface on the upper part of the ancient linear dunes.
Senegal-1001	Charcoal from a fireplace amidst pottery

sherds sticking slightly above the deflated surface on top of the ancient linear dune. The heat of the fire has bound the sand particles together somewhat strongly, with the result that this spot is a few centimeters higher than the surrounding surface.

RADIOCARBON DATES AND THEIR CALIBRATION INTO HISTORICAL YEARS

These two charcoal samples were dated at the Centre for Isotope Research of the University of Gröningen (the Netherlands), renowned for its high standards and precision in radiocarbon dating.

GrN-18238 - Senegal 1000:

Result dating in conventional radiocarbon year BP;
480±30 BP

This date was calibrated into historical years with the computer calibration program of Van der Plicht and Mook (1988), using the high precision calibration curve of Stuiver and Pearson (1986). A confidence level of 68.3% (1 sigma) yields the following result:

Range: 1416-1441 cal AD
Point date of highest relative probability with accompanying range: 1430 + 11/-14 cal AD

GrN-18239 - Senegal 1001:

Result dating in conventional radiocarbon year BP;
390±30 BP

This date was calibrated into historical years with the computer calibration program of Van der Plicht and Mook (1988), using the high precision calibration curve of Stuiver and Pearson (1986). A confidence level of 68.3% (1 sigma) yields the following result:

Range: 1446-1500 cal AD
Point date of highest relative probability with accompanying range: 1467 + 33/-21 cal AD

CONCLUSIONS AND RECOMMENDATIONS

Both archaeological sites (charcoal and pottery sherds) on top of the

linear dune date to the 15th century AD. Judged on the appearance of the charcoal and pottery sheds in relation to the deflated surface, it seems probable that the current phase of deflation of the ancient linear dune has only recently begun. It may in fact be the first serious erosion and deflation of the ancient linear dune since man occupied its surface in the 15th century AD. This preliminary conclusion may perhaps be substantiated with the help of aerial photographs from the area, taken in various years. Hence it is necessary to first study the earliest aerial photographs and subsequently follow the changes through time on later aerial photographs to the present

The large mollusc shells should also be dated with radiocarbon. The pottery sherds should be classified by an archaeologist specialized in the regions of West Africa. The sherds should be compared with other known pottery from the area dating to the same period in order to establish the culture to which these sites on the ancient linear dune belong.

A detailed paleoclimatic history should be compiled from the literature. Local archaeology and history, as well as climatic changes, should be correlated with dune landscape history in order to assess the possible effect of both climatic and anthropogenic influences on the Sahelian dune landscape of northern Senegal.

REFERENCES

Ahlbrandt, T.S. 1979. Textural parameters of eolian deposits. InA study of global sand seas, E.D. McKee (ed.), 21-51. Prof. Pap. U.S. Geol. Surv., no. 1052.

Bagnold, R.A. 1931. Journeys in the Libyan Desert, 1929 and 1930. Geogr. J. 78, 13-39, 524-33.

Bagnold, R.A. 1941. The physics of blown sand and desert dunes. London: Methuen.

Buckingham, E. 1914. On physically similar systems; Illustrations of the use of dimensional equations.Phys. Rev.4, 345-76.

Cermak, J.E. 1971. Laboratory simulation of the atmospheric boundary layer. Am. Inst. Aeron. Astron. J. 9, 1746-54.

Chepil W.S. 1958. Soil conditions that influence wind erosion. U.S. Dept. Agri. Tech. Bull. no. 1185.

Cook, N.J. 1978. Wind-tunnel simulation of the adiabatic atmospheric boundary layer by roughness, barrier and mixing device methods. J. Industrial Aerodynamics, 3, 157-76.

Cowdrey, C.F. 1967. A simple method for the design of wind tunnel velocity-profile grids. Aerodynamics Division, National Physical Laboratory, Aero Note 1055.

Danin, A. 1978. Plant species diversity and plant succession in a sandy area in the Northern Negev. Floral 67, 409-22.

Folk, R.L. 1968. Bimodal supermature sandstone: Product of the desert floor. Proc. 23rd Int. Geol. Cong. 8, 9-32.

Fryberger, S.G. and A.S. Goudie 1981. Arid geomorphology. Prog. Phys. Geog. 5, 420-8.

Glennie, K.W. 1970. Desert sedimentary environments. Developments in Sedimentology 14, Amsterdam: Elsevier.

Griffiths, . F. and K.H. Soliman 1972. The northern desert (Sahara), Chapter 3. In H.E. Lansberg (ed.), World Survey of Climatology, Climates of Africa. 10: 75-132.

Haynes, C.V. 1982. Great sand sea and Selima sand sheet, eastern Sahara:

Geochronology of desertification. Science 217, 629-33.

Holm, D.A. 1960. Desert geomorphology in the Arabian peninsula. Science 132, 1369-79.

Isyumov, N. and H. Tanaka 1980. Wind tunnel modelling of stak gas dispersion - Difficulties and approximations. In Wind Engineering, J.E.Cermak (ed.), 987-1001. Oxford: Pergamon Press.

Jensen M. 1958. The model-law phenomena in natural wind. Ingenioren (International Edition) 2, 121-28.

Kind, R.J. 1976. A critical examination of the requirements for model simulation of wind-induced erosion/deposition phenomena such as snow dritfing. Atmos. Env. 10, 219-27.

Kind, R.J. and S.B. Murray 1982. Saltation flow measurements relating to modeling of snowdrifting. J. Wind Engng. Ind. Aerodyn. 10, 89-102.

Kline, S.J. 1965. Similitude and approximation theory. New York: McGraw-Hill.

Mabbutt, J.A. 1968. Aeolian landforms in Central Australia. Aust. Geogr. Stud. 6, 139-50.

McKee, E.D. and G.C. Tibbitts 1964. Primary structures of a seif dune and associated deposits in Libya. J. Sed. Petrol. 34, 5-17.

Michel, P. 1980, The southwestern Sahara margin: Sediments and climatic changes during the recent Quaternary. In M. Sarnthein, E. Seibold and P. Rognon (eds.), Sahara and Surrounding Seas. 12: 297-306.

Mironer, A. 1979. Engineering fluid mechanics. New York: McGraw-Hill.

Pye, K. and H. Tsoar, 1990. Aeolian Sand and Sand Dunes. London: Unwin Hyman.

Simonett, D.S. 1960. Development and grading of dunes in Western Kansas.Ann. Assoc. Am. Geogr. 50, 216-41.

Stuiver, M. and G.W. Pearson 1986. High-precision calibration of the radiocarbon time scale, AD 1950-500 BC. In 12th International 14C Conference Proceedings (M. Stuiver and R.S. Kra), Radiocarbon Vol. 28, No. 2B, pp. 805-838.

Tsoar, H. 1976. Characterization of sand dune environments by their

grain-size, mineralogy and surface texture. In: Geography in Israel, D.H.K. Amiran and Y. Ben-Arieh (eds.), 327-43. Jerusalem: Israel National Committee, International Geographical Union.

Tsoar, H. 1978. The Dynamics of Longitudinal Dunes. Final Technical Report. London: European Research Office, U.S. Army.

Tsoar, H. 1983a. Dynamic processes acting on a longitudinal (seif) sand dune. Sedimentology 30, 567-78.

Tsoar, H. 1983b. Wind tunnel modeling of echo and climbing dunes. In Eolian sediments and processes, M.E. Brookfield and T.S. Ahlbrandt (eds.), 247-59. Amsterdam: Elsevier.

Tsoar, H. 1986. Two-dimensional analysis of dune profile and the effect of grain size on sand dune morphology. In Physics of desertification. F. El-Baz and M.H.A. Hassan (eds.), 94-108. Dordrecht: Martinus Nijhoff.

Tsoar, H. and J.T. Møller 1986. The role of vegetation in the formation of linear sand dunes. In Aeolian Geomorphology, W.G. Nickling (ed.), 75-95. Boston: Allen and Unwin.

Tsoar, H. and K. Pye 1987. Dust transport and the question of desert loess formation. Sedimentology 34, 139-53.

Van der Plicht, J. and W.G. Mook (1988). Calibration of radiocarbon ages by computer. Radiocarbon Vol. 31, No. 3.

Warren, A. 1972. Observation on dunes and bi-modal sands in the Tenere Desert. Sedimentology 19, 37-44.

White, B.R 1982. Two-phase measurements of saltating turbulent boundary-layer flow. Int. J. Multiphase Flow, 8, 459-73.

Wilson, I.G. 1973. Ergs. Sed. Geol. 10, 77-106.

Wood, W.H. 1970. Rectification of wind blown sand. J. Sed. Petrol.40, 29-37.

Appendices

LD/CND/N°080/CGF/CHAN/87

Le Consul Général du Sénégal à Paris

Paris, le 3 JUIN 1987

22, rue Hamelin, 75116 Paris

Tél. 505-75-86

Monsieur,

Suite à votre intervention auprès des services compétents du Consulat Général du Sénégal, nous portons à votre connaissance que rien ne s'oppose à la délivrance d'un visa d'entrée et de court séjour au Sénégal en votre faveur.

En conséquence, vous êtes invité à vous présenter auxdits services dès que vous le jugerez opportun.

Veuillez croire, Monsieur, à l'assurance de ma considération distinguée./.-

Pour le Consul Général et p.o.
Le Consul Général Adjoint

Ousmane BA

onsieur Haim TSOAR
enior Lecturer in Physical
éography Ben Gurion University
f the Negev
O BOX 653
EER-SHEVA 84 105
ISRAEL

Appendix 1: A letter from the Consul General of Senegal in Paris assuring Prof. Tsoar that he will get a visa to visit Senegal.

UNIVERSITE CHEIKH ANTA DIOP
DE DAKAR

Institut de Technologie
Nucléaire Appliquée(ITNA)

Le Directeur

Dakar, le 18 janvier 1990

To
HAIM TSOAR
Chairman & Senior Lecturer
BEN-GURION UNIVERSITY OF THE NEGEV

Dear Professor TSOAR,

Thank for your letter of 28 december 1989. The new dates are suitable for the visit. I have some difficulties to give the full financial plan of the trip. This planning depends on the inclusion or the exclusion of the definitive beginning of the project from the actual trip. So I indicate some proposals taking into account the maximal conditions you may expect for the ruling of the project. Detailed accounting will be made from the very beginning to the end of the programme for the needs of the reports we have to deliver to USAID.

PREVISION /

- 1 Car (for the fields) and all commodities	US 30 000
- Commodities equipment	US 700
- Commodities and Oil and management including Hotel.	US 10 000
- Risks garantee.	US 7 000
TOTAL .	US 47 700

These indications are maximum and you can revise them depending on your actual view of the present phase of the project without underestimating possible increase of the costs if the mangement is made without having in mind necessary initial conditions for the long term (3 years) of the programme. The period of march is very hot and possibly sandy in the region of Dagana. During the trip adelailed financial and operational plan will be outlined with Mrs BRUINS and FENIN.

Best wishes for the new year.
I hope to hear from you very soon and at your earliest convenience.

Christian-Sina DIATTA.

LE DIRECTEUR DE L'ITNA.
C. S. DIATTA

Appendix 2: A letter from Professor C.S. Diatta listing the expenses for field work that comes to the total of $47,000

Appendix 3: The X-ray diffraction results of grain surface coating shown in the photographs (Appendix 4).

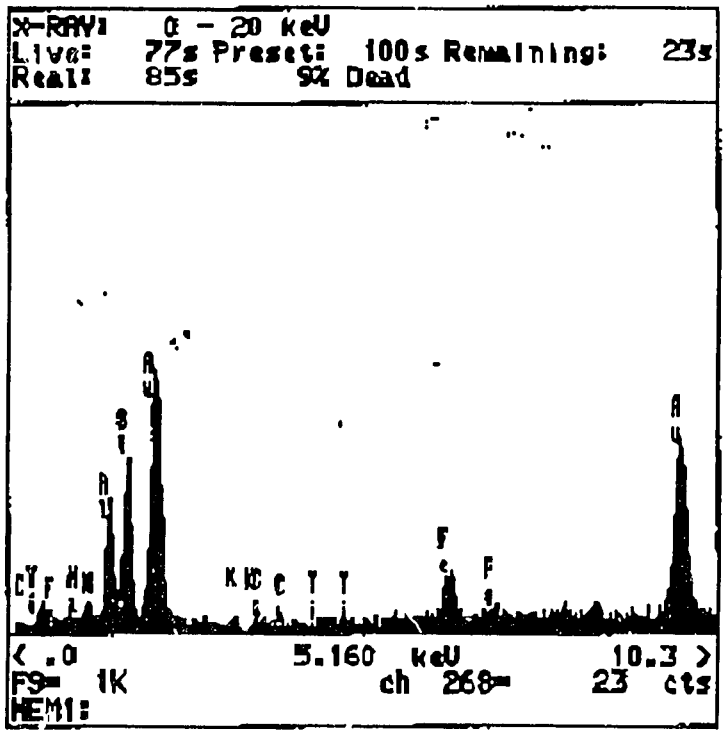

SE 46 - grain in photo # 15

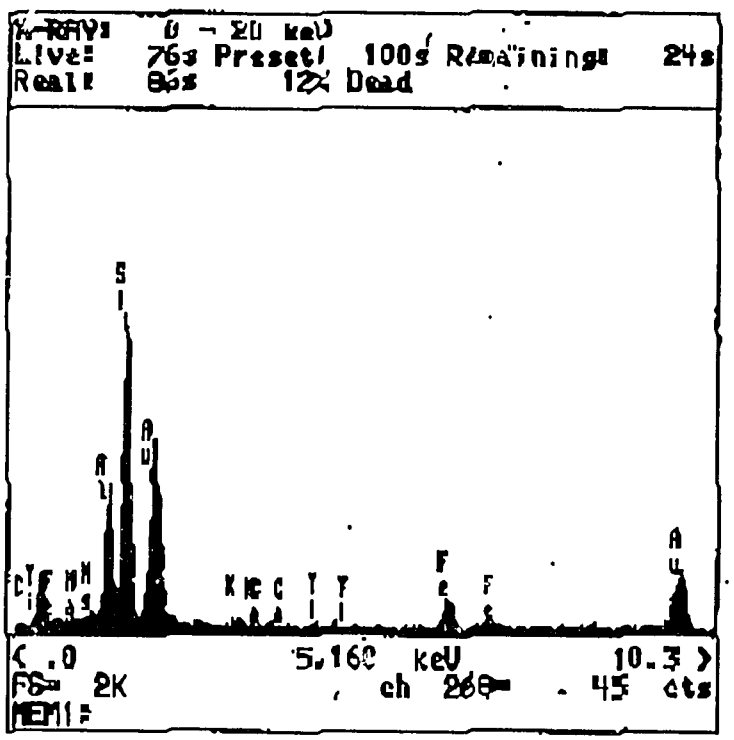

SE 46 - Analysis of all grains shown in photo # 14

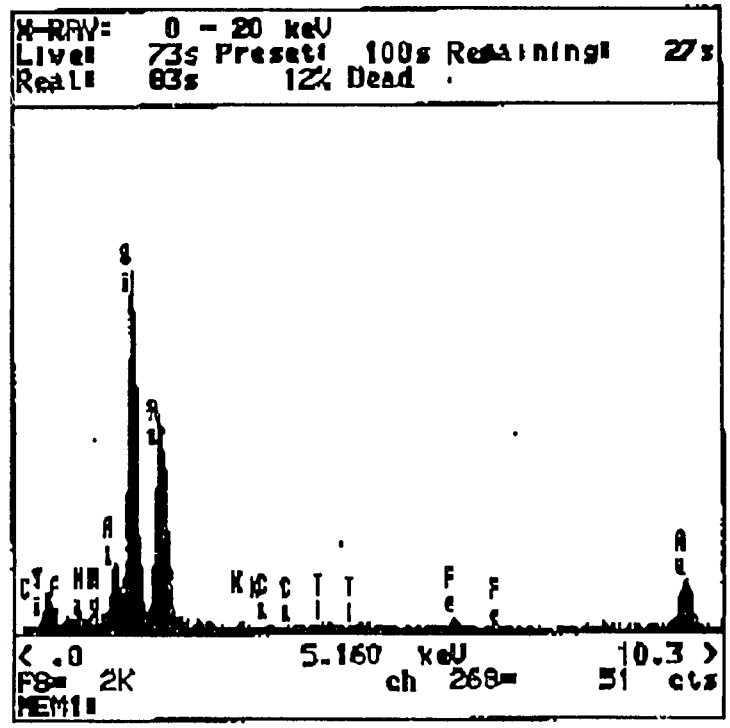

SE 30 - Analysis of all grains shown in photo # 7

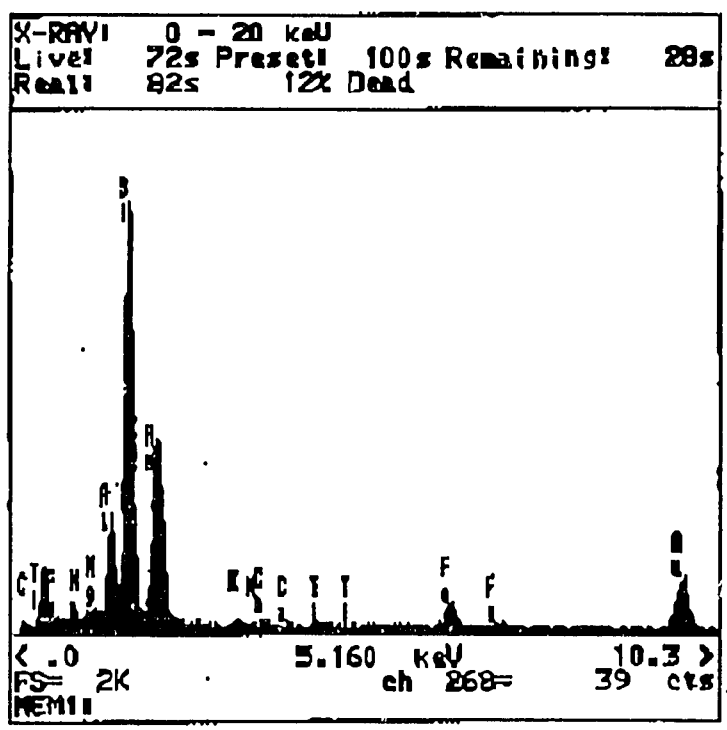

SE 75 - Analysis of all grains shown in photo # 26

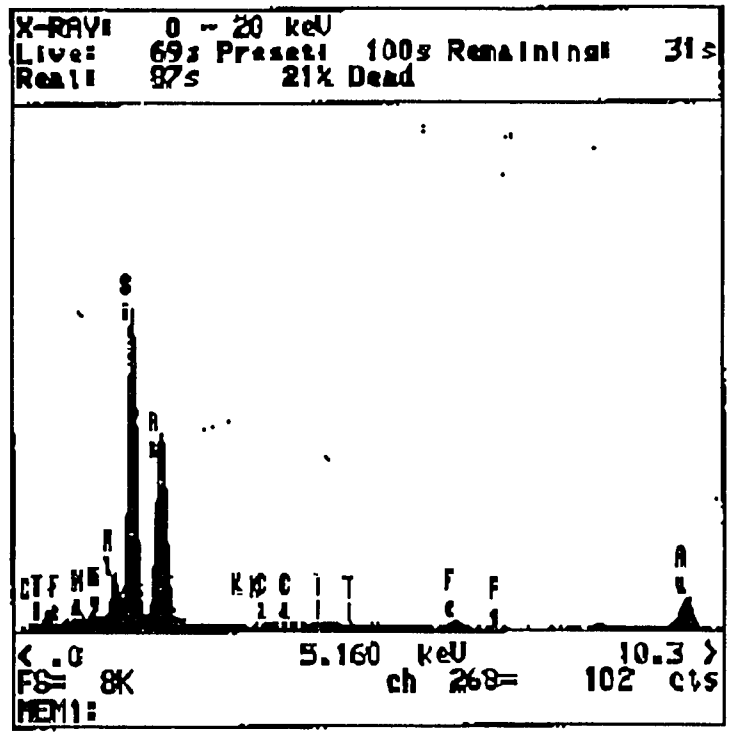

SE 34 - Analysis of grain shown in photo # 30

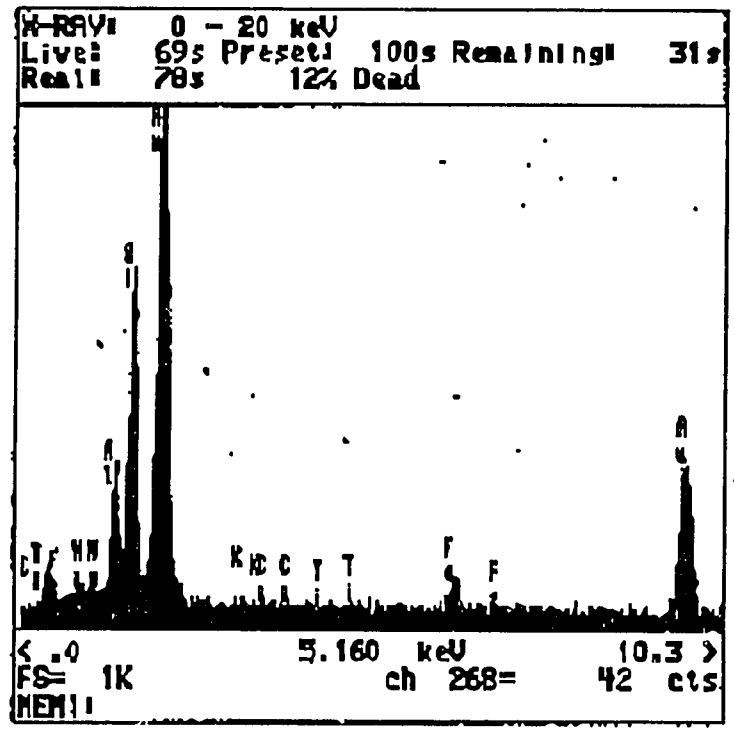

SE49 - Analysis of all grains shown in photo # 33

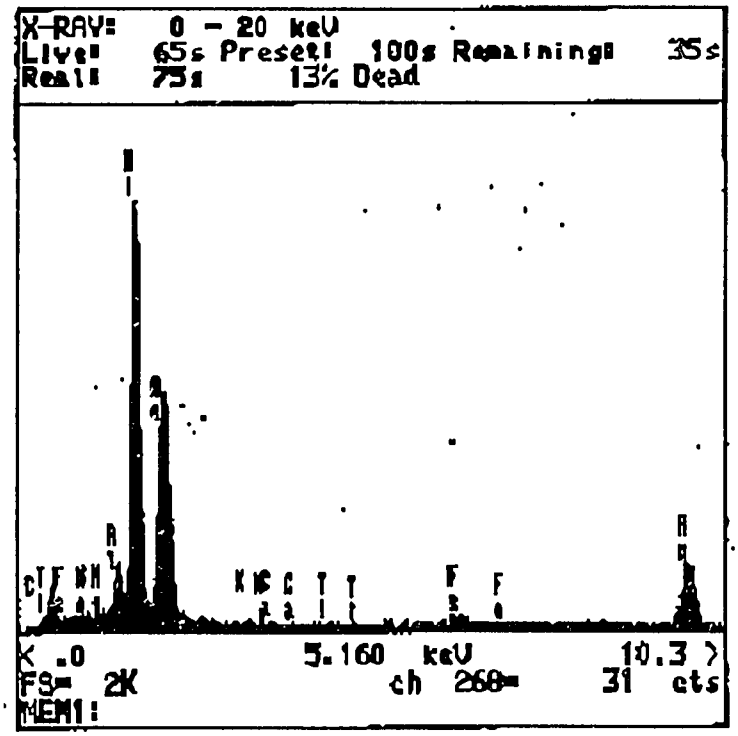

SE34 - Analysis of all grains in photo # 29

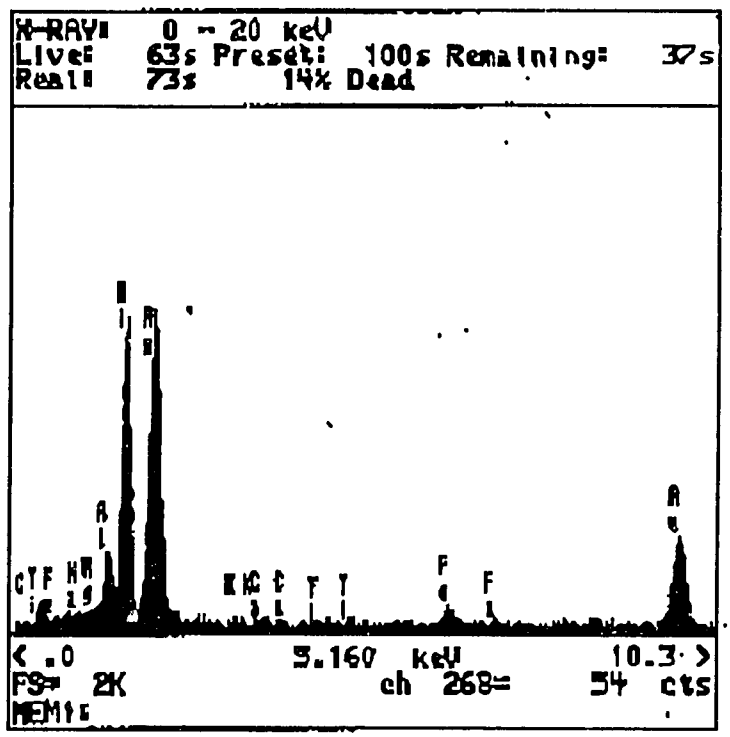

SE37 - Analysis of "coating" a grain in centre of photo # 21

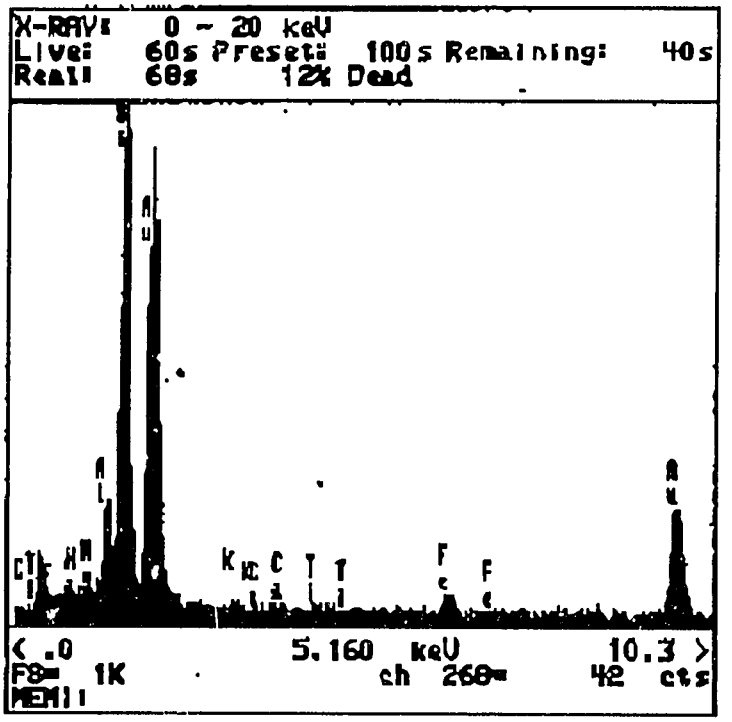

SE 22B - Analysis of all grains in photo # 22

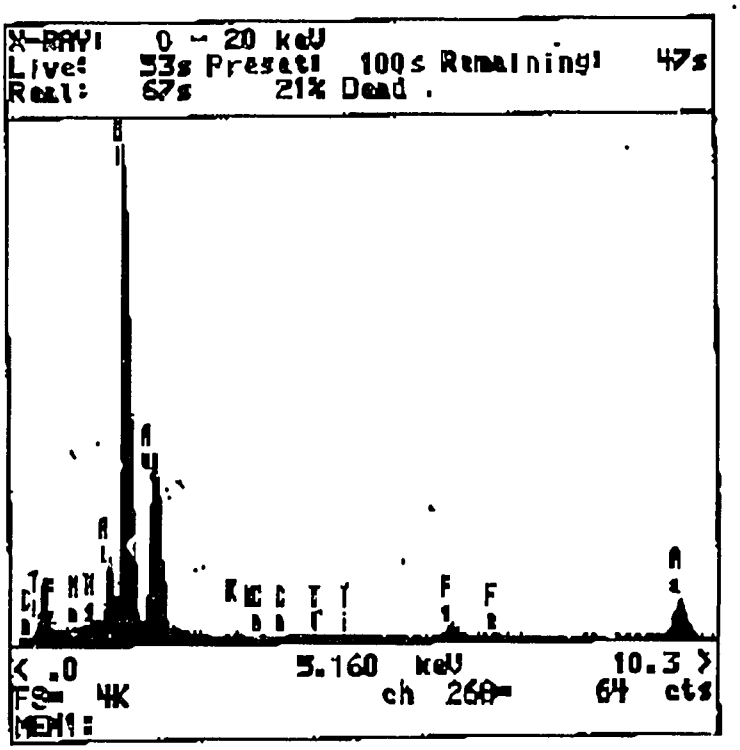

SE 24 - Grain shown in photo # 3
- quartz with aluminiosilica - Fe oxide coating

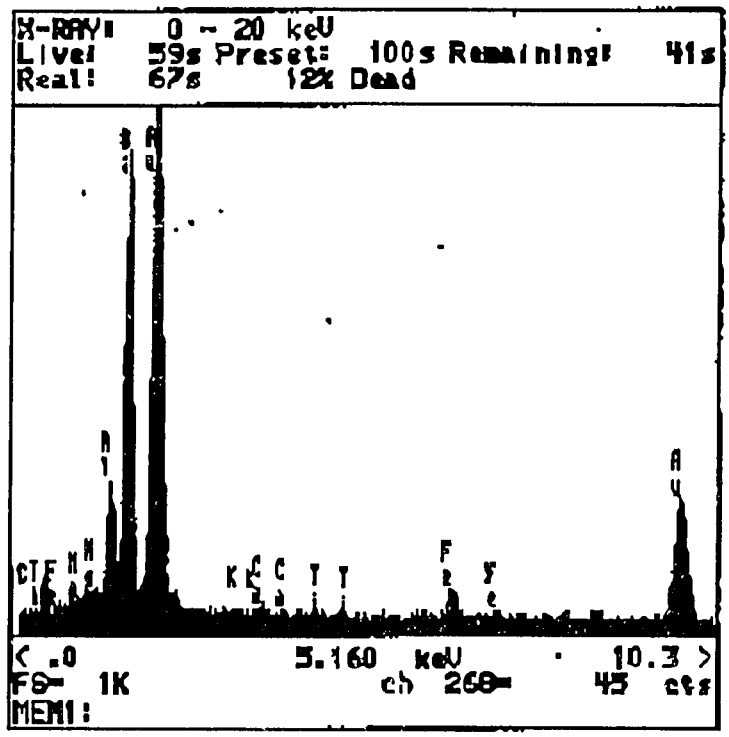

SE 37 - Analisis of grains in photo # 17
(quartz with alumino-silica Fe oxido coating)

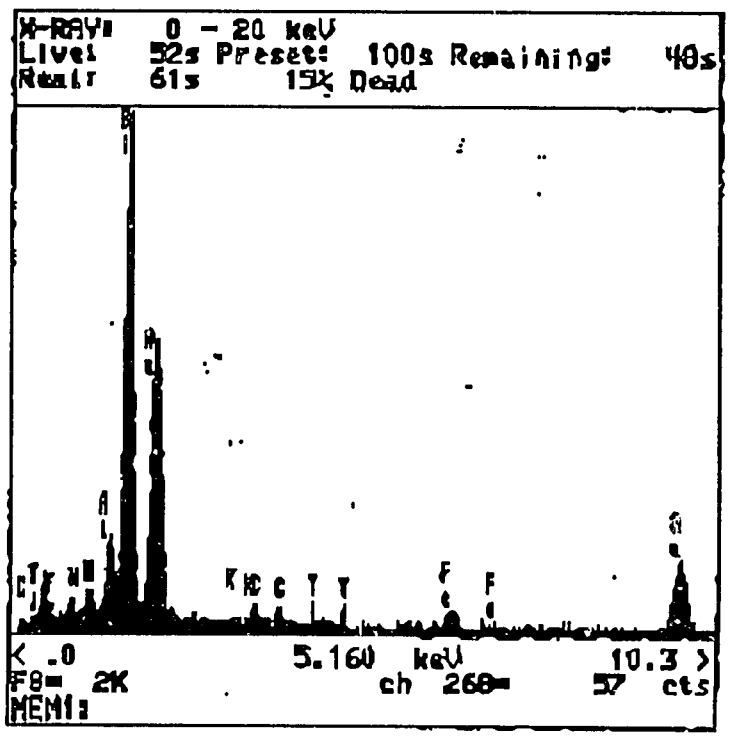

SE 22B - Analysis of grain surface shown in
photo # 24

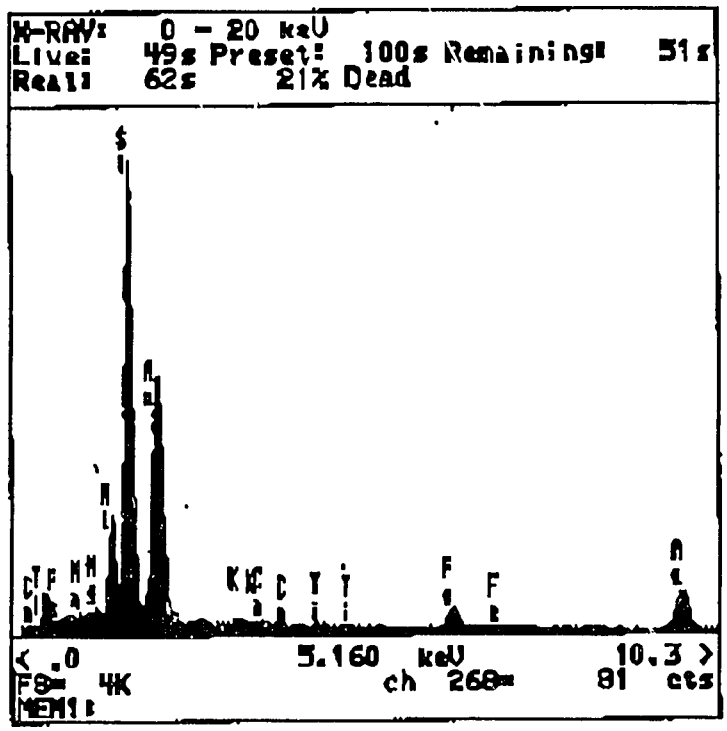

SE 24 - Grain surface coating in photo # 5

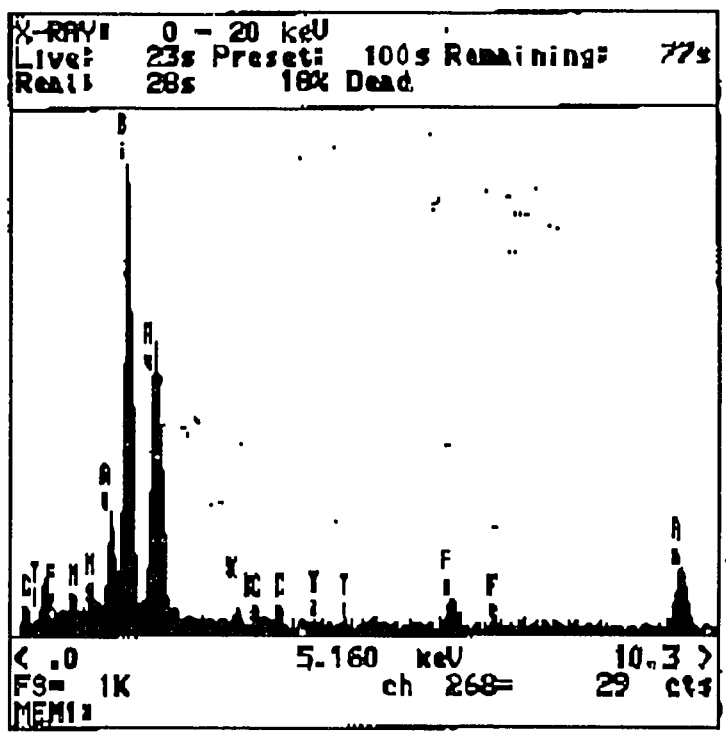

SE 24 - Grain photo # 4 quartz with aluminio-silica - Fe-oxide coating; posible incorperating some clay minerals

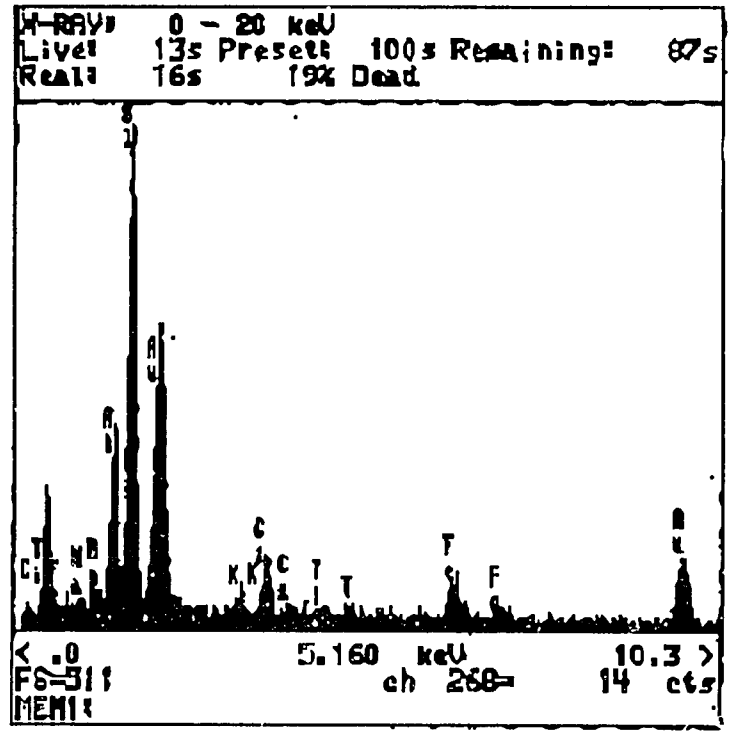

SE 75 - Analysis of agregate grain shown in photo #27

Appendix 4: The SEM photographs of the grains on which X-ray diffraction analyses of the surface coating have been done.

*SE 24
Brown sand from paleosol layer
in linear dune section

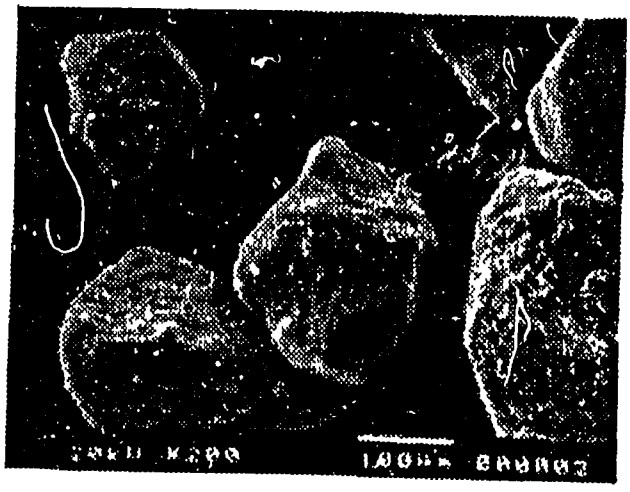

* SE 24

* SE 24

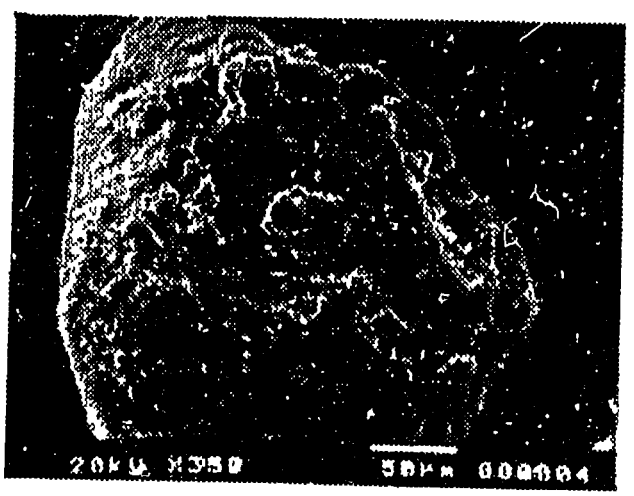

*SE 24

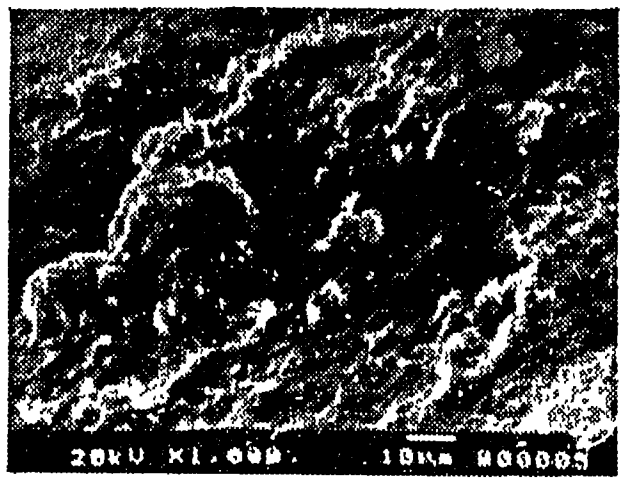

* SE 24

* SE 24

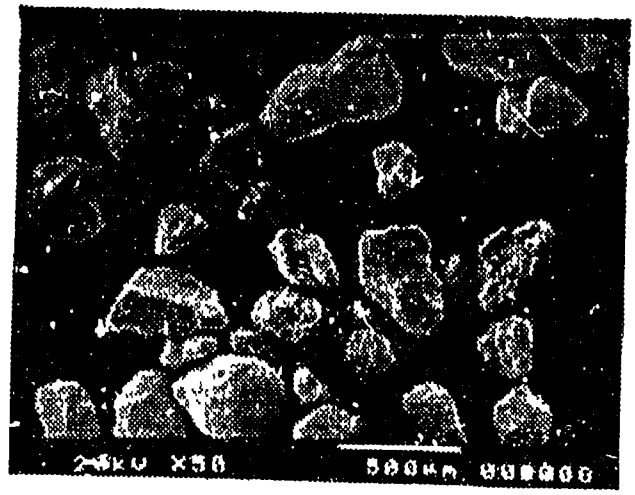

*SE 30
Yellow-pale orange sand
from linear dune section

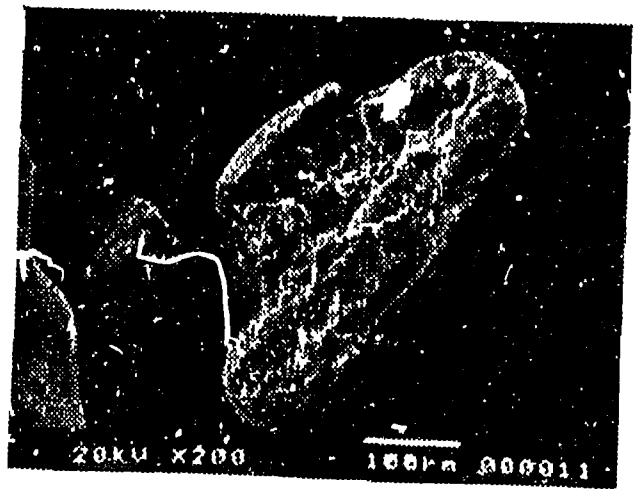

*SE 30

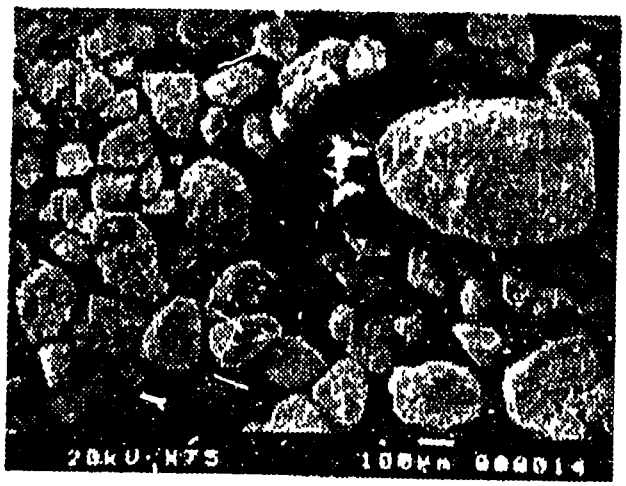

* SE 46
Sand sheet
dark reddish orange

*SE 46

* SE 46

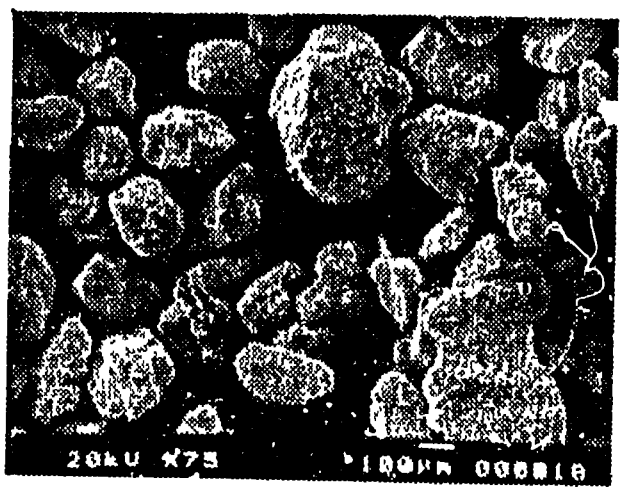

* SE 37
Gleyed layer at base of linear dune profile - reddish orange

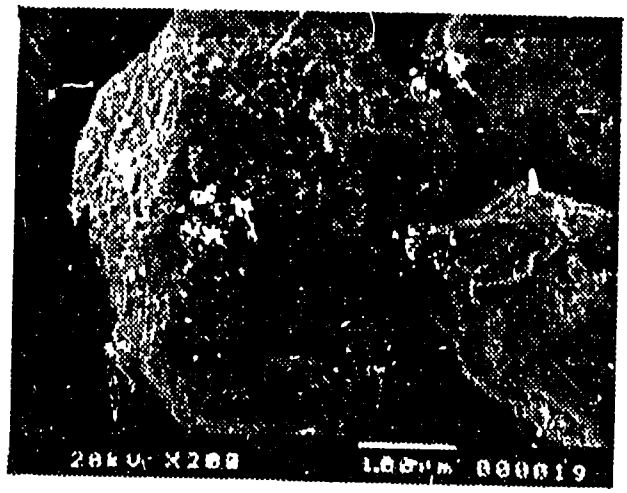

* SE 37

* SE 37

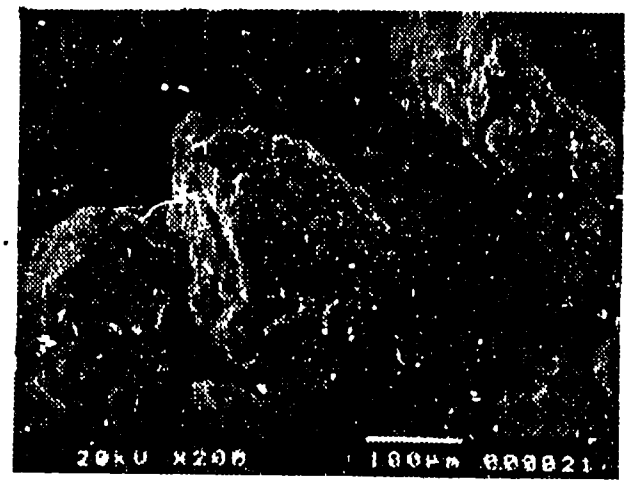

#SE 37

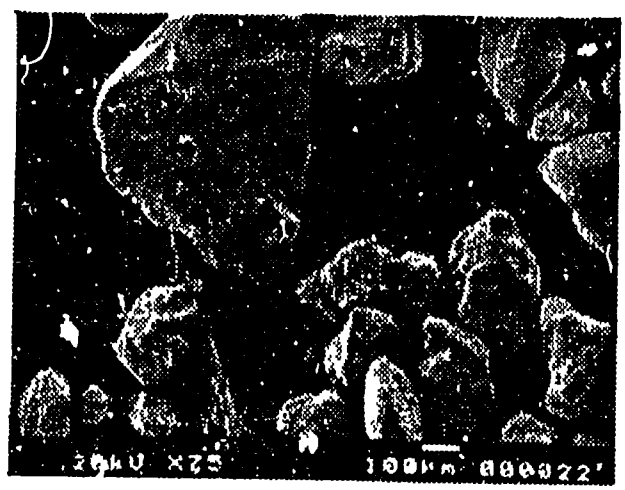

#SE 22B
Top of paleosol layer,
linear dune section-brown (dark)

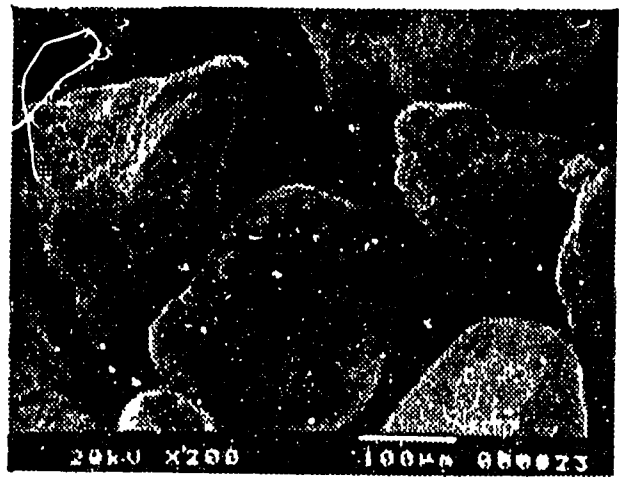

#SE 22B

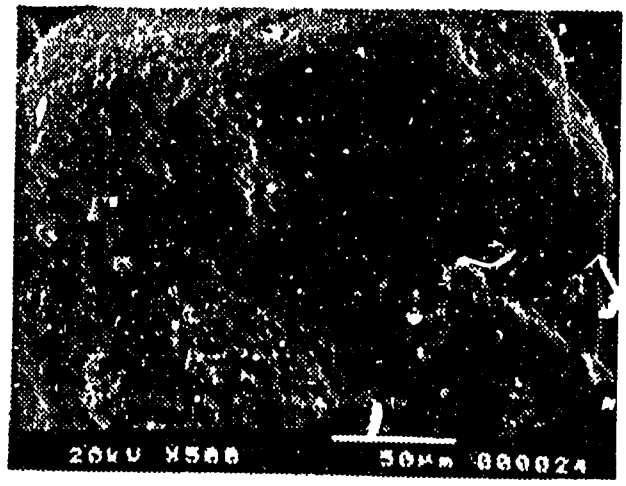

SE 22 B

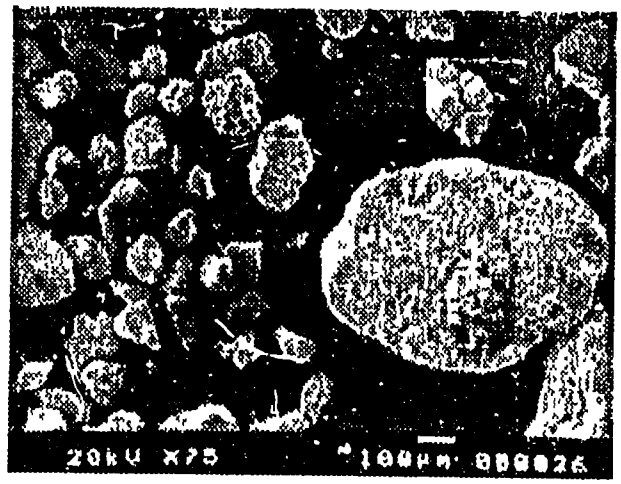

*SE 75
Brown sand-burned paleosol A horizon
in sand sheet sequence

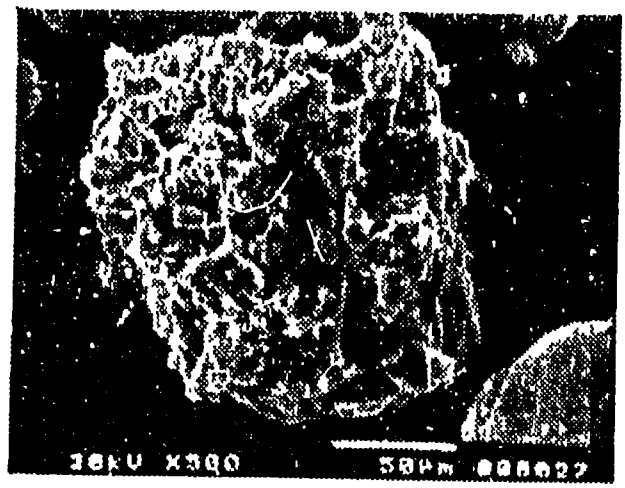

* SE 75
Grain aggregate

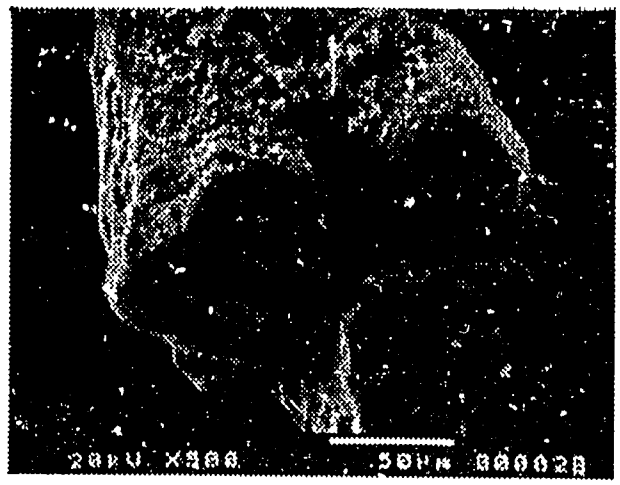

#SE 75
Loosely cemented grain aggregate

#SE 34
Gleyed layer near base of
linear dune section-orange

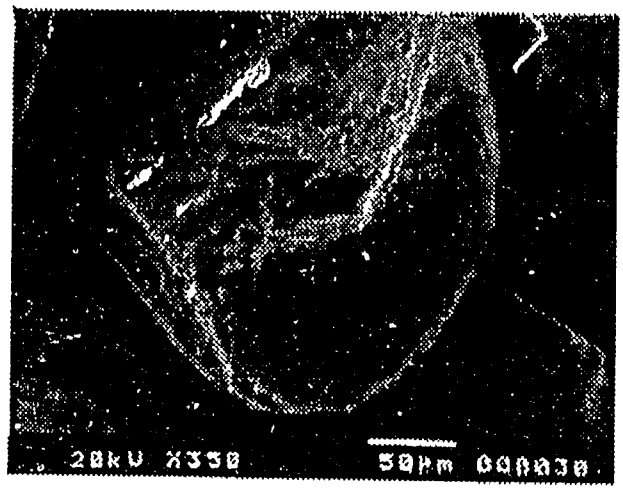

* SE 34

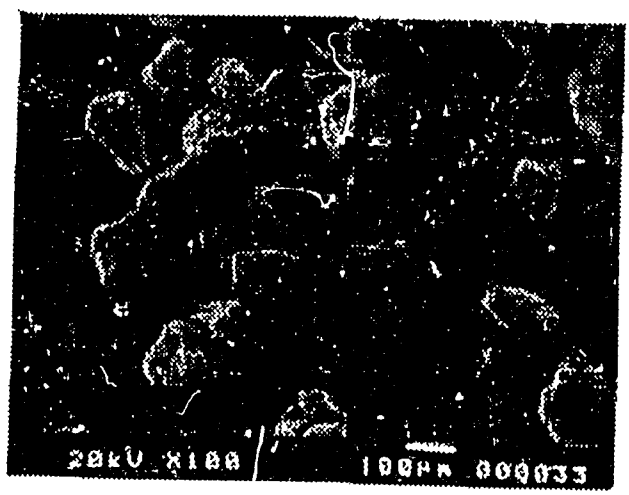

*SE 49
Reddish-orange bimodal sand
in sand sheet sequence

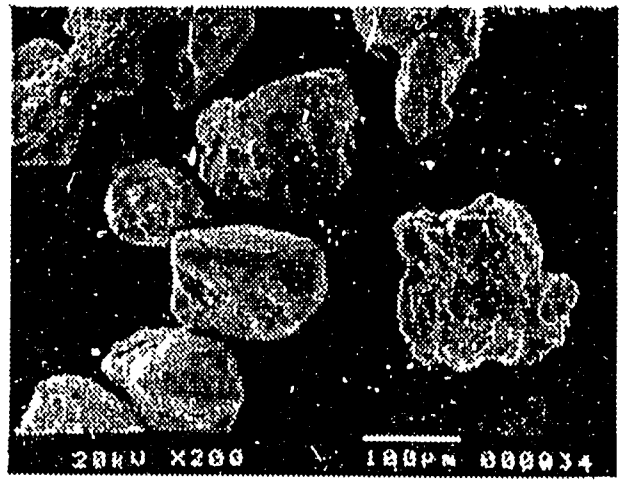

SE 49

SE 49

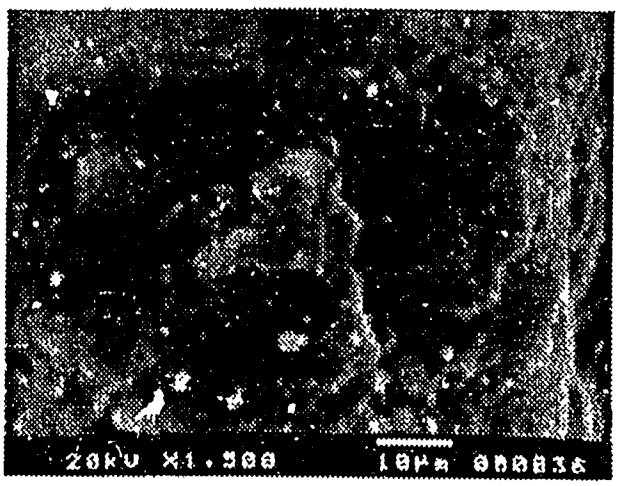

* SE 49

PN-ABQ-103
C7-143 84915

I-GURION UNIVERSITY OF THE NEGEV
3. 653 BEER-SHEVA, 84105, ISRAEL

אוניברסיטת בן-גוריון בנגב
ת.ד. 653 באר-שבע 84105

FINAL

8 June 1993

83069

Dr. Miloslav Rechcigl
Office of the Science Advisor - US-Israel CDR Program
AID/SCI, Room 320, SA-18
Agency for International Development
320 Second Street
Washington, D.C. 20523-1818
U. S. A.

Dear Dr. Rechcigl:

Re: Grant No. DPE-5544-G-SS-7036-00
Bimodial Eolian Desert Sand Sheets
Prof. Haim Tsoar - BGU / Prof. K. Anane Fenin - Ghana

Enclosed please find three copies of the final scientific report submitted by Prof. Haim Tsoar for the above-mentioned project.

Thank you for your cooperation and support of this research.

Yours sincerely,

Moshe Amir
Director
Department of Research Contracts

cc: Dr. D. Mulenex - US Embassy, Tel-Aviv (w/encl)
PPC/CDIE - (w/encl)
Prof. H. Tsoar

CC-C DIE + BUSTID

JUN 22 1993

RCH & DEVELOPMENT AUTHORITY
ent of Research Contracts
461701, 76772 :טל | Facsimile 057-37757 | Telex 5379/BGUCC ATT RESCO | Decnet BGUVMS RESCO | Bitnet

ר למחקר ולפתוח
ר מחקר

82